American
Petroleum
Institute

Smart Leak Detection and Repair (LDAR) for Control of Fugitive Emissions

Regulatory Analysis & Scientific Affairs
June 2004

Smart Leak Detection and Repair (LDAR) for Control of Fugitive Emissions

Regulatory Analysis & Scientific Affairs
June 2004

American Petroleum Institute
1200 L Street, Northwest
Washington, DC 20005

Prepared by:

ICF Consulting, Inc.
9300 Lee Highway
Fairfax, Virginia

Table of Contents

Smart Leak Detection and Repair (LDAR) for Control of Fugitive Emissions

Executive Summary

The Smart LDAR project is aimed at developing more efficient procedures and technologies for the control of fugitive emissions from process piping components (e.g. valves, pumps, connectors, etc.). A large refinery in the U.S. can spend over $1MM annually in monitoring, control measures, record keeping and reporting. Most of this effort appears to be wasted, since the vast majority of piping components (generally over 98%) do not leak. A recent API study showed that over 90% of controllable emissions come from about 0.13% of the components. A Smart LDAR program would focus efforts on these high leaking components.

This report presents a summary of the Smart LDAR concept, potential technologies, plant demonstrations and laboratory test results. Smart LDAR focuses on locating and repairing the most significant leaking components more cost effectively than existing practices while providing environmental protection equivalent or better than the current programs. While current LDAR programs have been successful in identifying and significantly reducing fugitive emissions from regulated components at industrial facilities, they are time consuming, labor intensive and costly. An operator must visit and measure each potential leak site; of which there are hundreds-of-thousands at an industrial plant. A Smart LDAR program that focuses on finding and repairing this minority of high "leakers" could achieve equivalent or better environmental protection at a lower cost.

Emerging optical imaging technologies provide a tool to more quickly identify high leaking components. Laser-based optical imagers have been identified. Remote sensing and instantaneous detection capabilities of these laser-based optical imaging technologies allow an operator to quickly scan large areas containing tens to hundreds of potential leaks. Significant leaks are identified immediately, allowing quicker repair, and ensuring efficient use of resources.

Monte Carlo Analyses have been performed to determine control equivalence for the optical imaging technology compared to current methods (i.e. EPA Reference Method 21). Environmental benefit equivalent to the current work practice is demonstrated when Monte Carlo simulations show that emission reduction for an alternative technology is the same as, or larger than, the current work practice emission reduction. In current fugitive emission control programs, quarterly monitoring is usually required for most components with leak definitions of 10,000 ppmv, 1,000 ppmv or 500 ppmv. Pumps are monitored monthly. The Monte Carlo analyses showed that for valves, optical imaging used at bi-monthly monitoring frequency, provides greater environmental protection than the current Method 21 quarterly monitoring.

Field and laboratory tests of optical imaging technologies have been conducted to demonstrate that the technologies could detect fugitive emissions at refineries and chemical plants under normal operating conditions and to determine detection limits. The project has been a cooperative effort of the petroleum industry, government funded laboratories, the U.S. EPA, and technology vendors.

ES-1.0 The Basis of Smart LDAR

In 1997, the American Petroleum Institute (API) conducted a study[1] to identify opportunities for conducting LDAR programs in a more cost-effective manner. The study evaluated data collected over more than 5 years at 7 Los Angeles, California refineries in the South Coast Air Quality Management District (SCAQMD). The data were examined to help determine if there were any design or operational characteristics that influence fugitive emissions, and whether a focused LDAR program could be more cost effective at controlling these emissions compared to the current method.

The API Study showed that 84 percent of the refinery fugitive emissions were from high leakers (>10,000 ppmv), which were only 0.13 percent of the total number of components (See Figure ES-1)[2]. Of the remaining 16 percent of the estimated emissions, 9.5 percent were from non-leakers (screening <100 ppmv), which constitute 99 percent of the components, and whose estimated emissions are based primarily upon an EPA specified, "zero default," value for components that screen at the background concentration. Thus, the high leakers account for 92 percent of the controllable (i.e., non-default zero) emissions.

Figure ES-1: Distribution of Component Count and Estimated Emissions by Screening Range

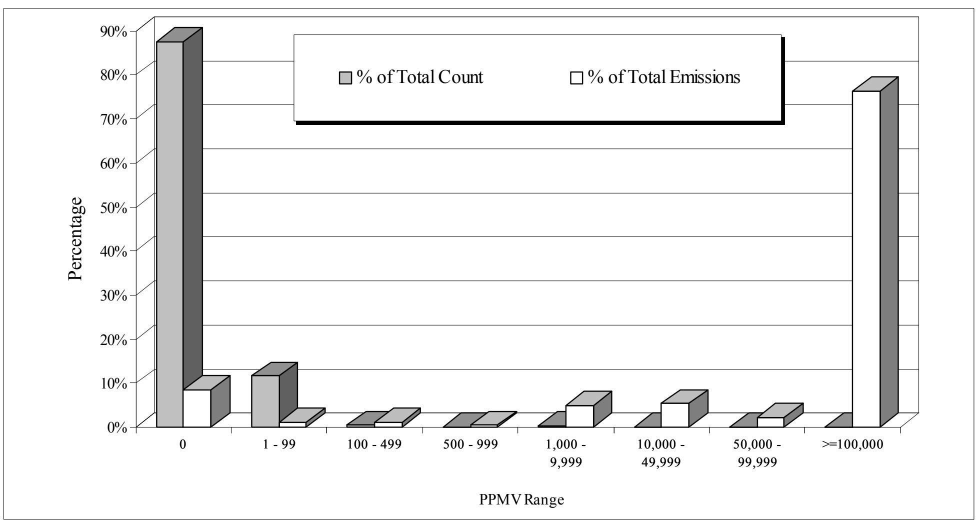

The study also found that there were no chronic leakers and only 5.4 percent of all emissions were from repeat leakers. Instead, the high leakers were found to occur randomly. No systematic explanation for their occurrence was apparent. The Study concluded that a more cost effective LDAR program would be one that emphasizes the location and repair of high leakers. The API has named such a program Smart LDAR.

ES-2.0 Optical Imagers for Locating Leaking Components

Two technologies have been tested at plants by the API led work group and have successfully found leaking components:

---

1 American Petroleum Institute, "***Analysis of Refinery Screening Data,"*** Publication # 310, Washington, DC, November 1997.

2 The overall percentage of high leakers (screening∃10,000) in any of the seven refineries was less than 0.2 percent.

- A CO_2 laser imager. This is a commercially available instrument, manufactured and marketed by Laser Imaging Systems (LIS) under the brand "Gas Vue®." Gas Vue® utilizes a CO_2 laser. The Gas Vue® was successfully tested at two chemical plants and is referred to as a CO_2 laser imager throughout this report.

- A "fiber" laser imager. This instrument, developed by Sandia National Laboratory's (SNL) Lawrence Livermore facility, utilizes a backscatter technique patented by LIS. It is referred to as a "fiber" laser in reference to its optical fiber laser amplifier. It was successfully tested at two refineries and a chemical plant.

Each laser is tuned to emit a specific wavelength of infrared light that provides specific compound or compound type detection. The CO_2 laser is discreetly tunable in the 8-10 micron spectral region. The fiber laser is continuously tunable in the 3 micron spectral region.

ES-2.1 Backscatter Absorption Gas Imaging (BAGI)

The principle of operation of the CO_2 laser and fiber laser is Backscatter Absorption Gas Imaging (BAGI). In BAGI, a live video image is produced by illuminating the view area with laser light in the infrared frequency range. The reflected (backscattered) laser light is detected with a camera sensitive to that light. When the chosen laser wavelength is strongly absorbed by the gas of interest, a cloud of that gas is revealed as a dark image as shown in Figure ES 2-1.

A video camera-type scanner both sends out the laser beam and picks up the backscattered infrared light. The camera converts this backscattered infrared light to an electronic signal, which is displayed in real-time as an image on both the viewfinder and a video monitor. The same image will be seen whether the scanning is done in daylight or at night because the scanner is only sensitive to illumination coming from the infrared light source, not the sun. The imager can be switched between visible and infrared views.

Figures ES 2-2 and ES 2-3 show the visible light and infrared views of leaking components viewed with the CO_2 and fiber lasers.

Figure ES 2-1. Schematic Description of BAGI Process

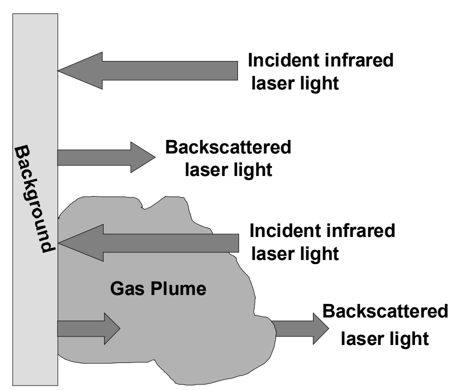

Source: As Adapted from McRae, Tom, *GasVue: A Rapid Leak Location Technology for Large VOC Fugitive Emissions*. (Presentation at the CSI Petroleum Refining Sector Equipment Leaks Group, Washington, DC, Sept. 9, 1997). See U.S. Patent # 4,555,627.

Note: Although this Figure shows the gas in contact with the background material, it is not a requirement that the gas be in contact with the background. The gas plume need only be between the background and the infrared camera.

Figure ES 2-2. CO_2 Laser Views of a Leaking Connector in Visible and Infrared Light

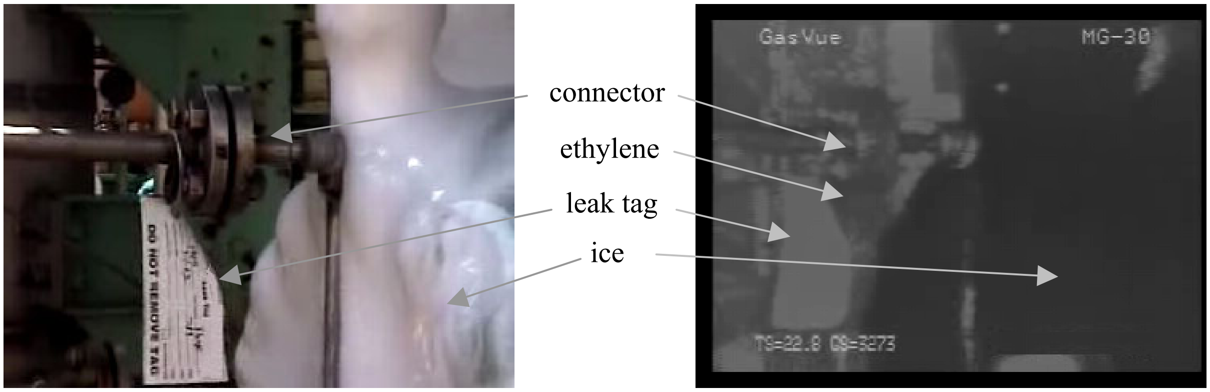

Figure ES 2-3. Fiber Laser Views of Leaking Flange in Visible and Infrared Light

Visible light view of leaking flange **Infrared view of leaking flange**

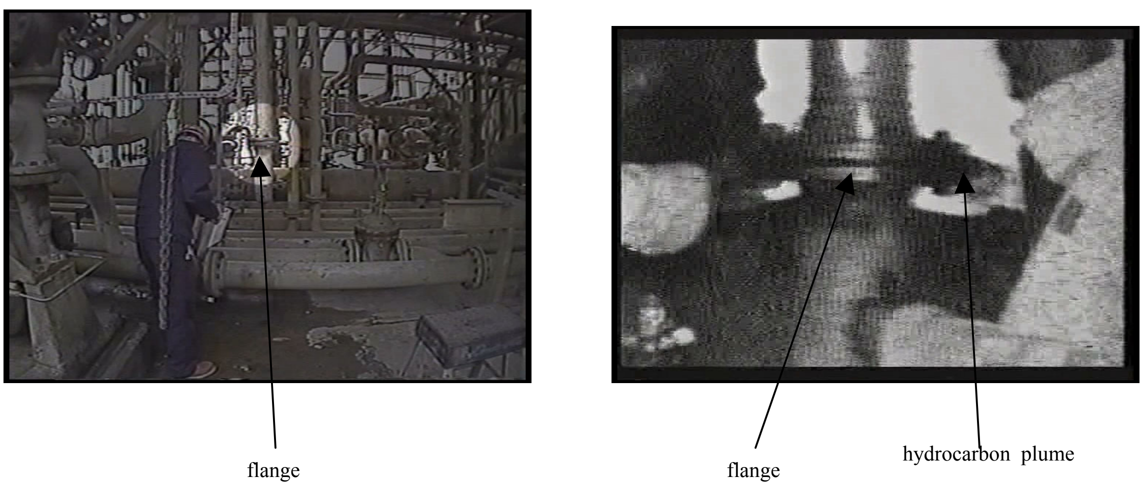

ES-3.0 Variability in Method 21

There is significant variability in EPA Reference Method 21. As shown in Figure ES 3-1, for a fixed mass rate, the screening value can range over several orders of magnitude. This uncertainty in Method 21 leads to bottom false positives and false negatives when compared to regulatory leak limits.

False negatives from Method 21 can result in significant emissions because these components would not be repaired and would continue to leak under a Method 21 based program. Since these components would be identified as leakers by the optical imaging instrument, the reduction of these emissions, which were “missed” by Method 21, is a major advantage for using the optical imaging technology. Thus, the new Smart LDAR approach using optical imaging allows a much higher mass leak definition than when using Method 21 since these missed leaks (the false negatives) are found and repaired more frequently.

In the current fugitive emission control program required by U.S.EPA regulation, monthly monitoring is required for pumps and quarterly monitoring is required for other components with leak definitions for repair of 500, 1,000 and 10,000 ppmv. Less frequent monitoring is allowed if the percent of leaking components remains below a specified level for a specified number of periods. Lower leak definitions for repair do not necessarily lead to better emissions control since, as the leak level is decreased, few additional leaking components are added to the repair group and these contribute very little to the overall mass emissions.

Figure ES 3-1. Variability of Method 21 Results for Equivalent Mass Emission Rates

Note: In a box plot, boxes enclose the middle half of the data spread, from the 25th to the 75th percentiles, with a horizontal line drawn inside the box at the median (50th percentile) value; whiskers extend below the box to the 5th percentile value and above the box to the 95th percentile value; and "dots" indicate values smaller than the 5th percentile value or larger than the 95th percentile value.

This illustration shows box plots for 1993-94 Petroleum Industry bagging data-set (American Petroleum Institute, 1993a; 1993b; and 1994) depicting reported screening value ranges (ppmv) for different "levels" of mass emission rates, denoted by mass magnitude bins (e.g., mass emission rate magnitude "1E-8" indicates mass emission rates with units of 10^{-8} kg/hr; i.e., values 1H10^{-9} kg/hr or larger, and less than 1H10^{-8} kg/hr, because the integer portion of the base-10 logarithm for values between these bounds is "-8")

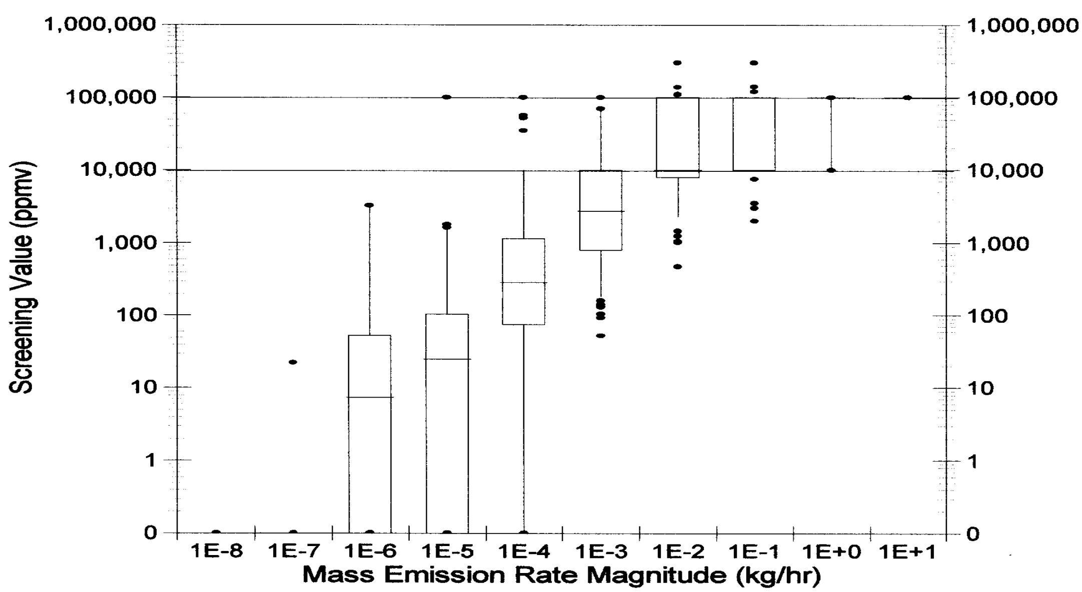

The Smart LDAR approach focuses on identifying and repairing the highest leakers since these are the source of almost all the mass emissions. Equivalence is obtained by more quickly finding and repairing these large leaks, which more than off-sets the emission rates from components with low ppmv readings that leak for longer periods under current guidelines. Figure ES 3-2 illustrates the concept that Smart LDAR (on average) finds large leaks in shorter time, while the current approach (on average) finds smaller leaks over longer time. The total emission is equal under both approaches but more cost-effective

Figure ES 3-2. Equivalence From Quicker Repair of Highest Leakers

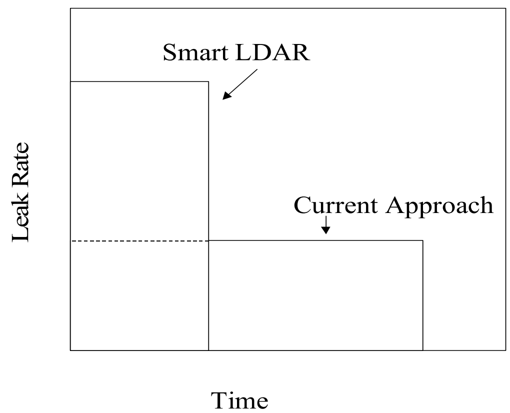

Note: Not drawn to scale.

using the Smart LDAR approach. The use of optical imaging provides a more cost effective approach to more quickly find the high leakers. This, combined with the potential to find the false negatives (missed high leakers) from the Method 21 approach, results in the benefits from the Smart LDAR technique using the optical imaging technology.

ES-4.0 Testing and Demonstrating Applicability of Optical Imaging

Several field and laboratory studies have been conducted to demonstrate the use of optical imaging for fugitive emissions monitoring. These studies, their purpose and overall outcomes are summarized in Table ES 4-1.

Table ES 4–1. Laboratory and Field Tests and Demonstrations of the Fiber- and CO_2 Lasers

Test/Year	Purpose	Outcome	Chapter for Details
Refinery Demonstration of Van-mounted Fiber Laser Technology, 1999	Determine if fiber laser could detect aliphatic emissions at a refinery under normal operating conditions.	Successfully detected leakers.	Chapter 6
Laboratory Tests of Portable Fiber Laser, 2000	Explore influence of viewing distance, wind speed, leak rate, reflective background, on the performance of the instrument in a controlled environment.	Data obtained on mass rate detection threshold for controlled wind speed, distance and reflective background. The lowest detected leak was at 8 g/hr[3] seen from 10 ft away at wind speed of 1 m/s.	Chapter 7
Laboratory Tests of Portable Fiber Laser, 2001	Determine the influence of viewing distance, wind speed, mass leak rate, reflective background, on the detection thresholds in: (1) a controlled wind-tunnel and (2) in out-door test with "blind" elements	Test determined the leak detection threshold of the fiber laser. Lowest detected leak was about 0.2g/hr.	Chapter 8
Ethylene Chemical Plant Demonstrations of CO_2 Laser, 2002	Test whether the CO_2 laser can detect fugitive emissions at ethylene plants under normal operating conditions.	CO_2 laser successfully detected leaks from components with a mass leak rate greater than 1 g/hr.	Chapter 10
Refinery Test of Fiber laser, 2003	Test whether the fiber laser can detect fugitive emissions at a refinery under normal operating conditions	Fiber laser successfully detected leaks from components with a mass leak greater than 20 g/hr.	Chapter 9

ES 4-2. Laboratory Testing of Fiber Laser

The results of the laboratory testing (wind tunnel and out-door roving tests) of the fiber laser for all conditions are shown in Figure ES 4-1. As shown in the plot, the mass rate detection threshold exceeded 10 g/hr in only 10 cases. Seventy-three percent of the mass detection thresholds determined in the lab test were below 5 g/hr.

[3] Leak rate set at test component.

Figure ES 4-1. Minimum Detected Mass Flow Rate for all Leak Conditions under Laboratory Testing

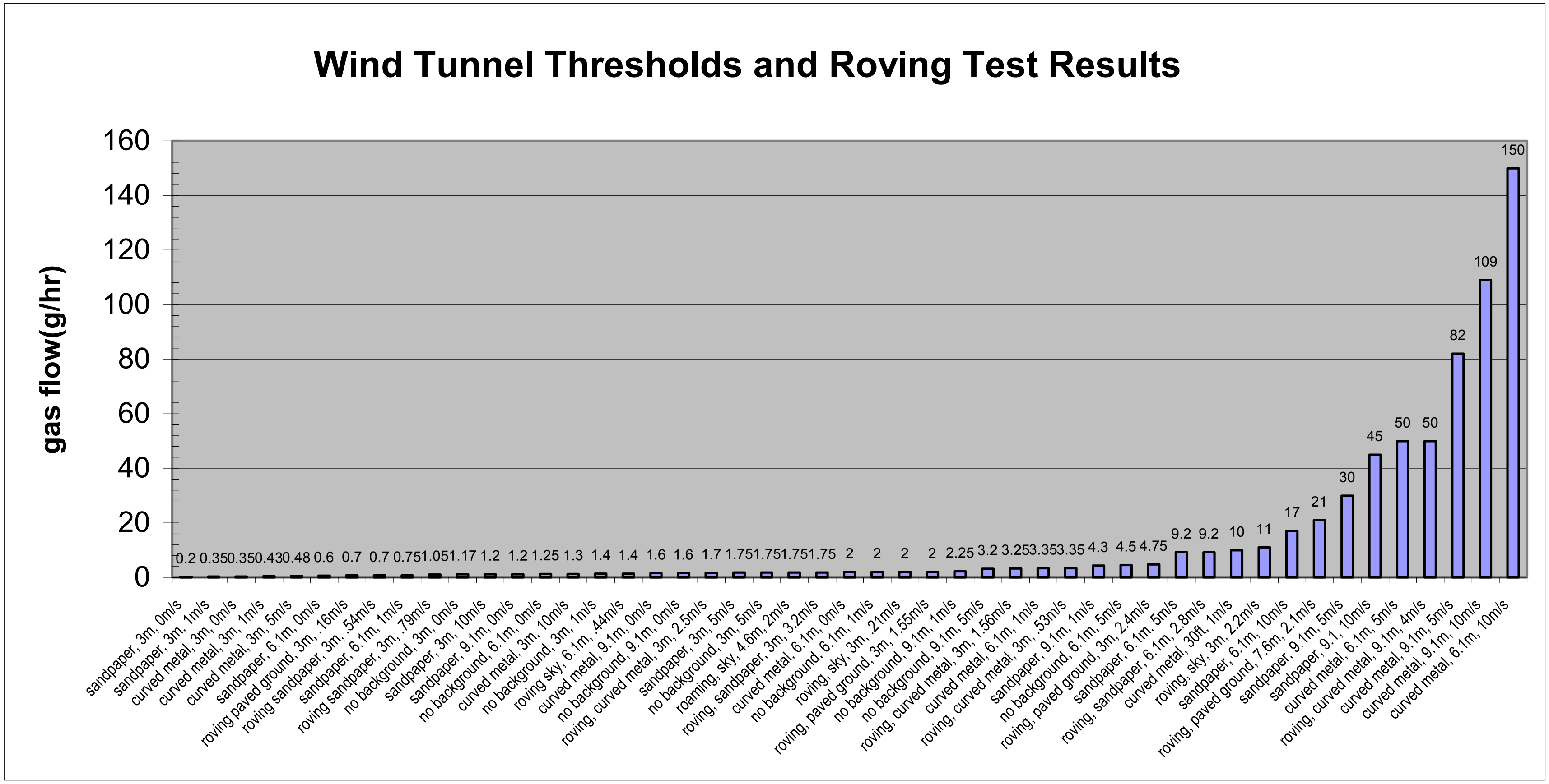

Results of refinery testing with the fiber laser showed that the imager detected all leaks above 20 g/hr (see Figure ES 4-2). The mass leak rates were determined with bagging analysis. Below 20 g/hr, the fiber laser detected roughly 50 percent of the leaks. Some leaks at lower mass rates were detected when a background was added behind the gas cloud.

Figure ES 4-2. Fiber Laser Performance at Refinery during 2003 Testing[4]

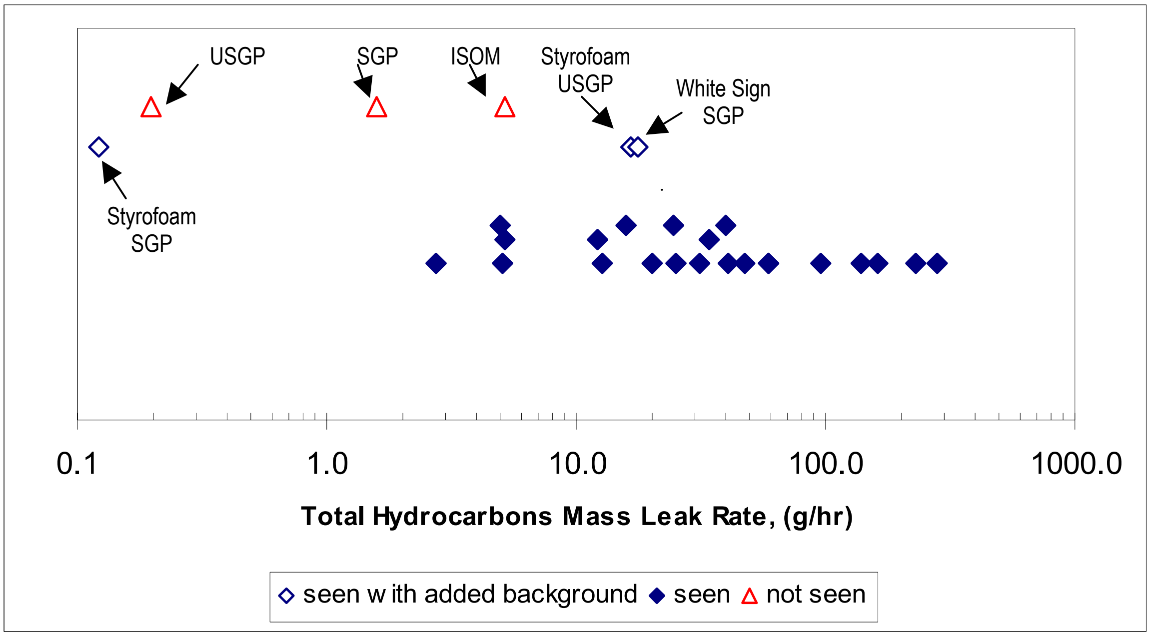

Figure ES 4-3. Scanning Refinery Components with Fiber Laser

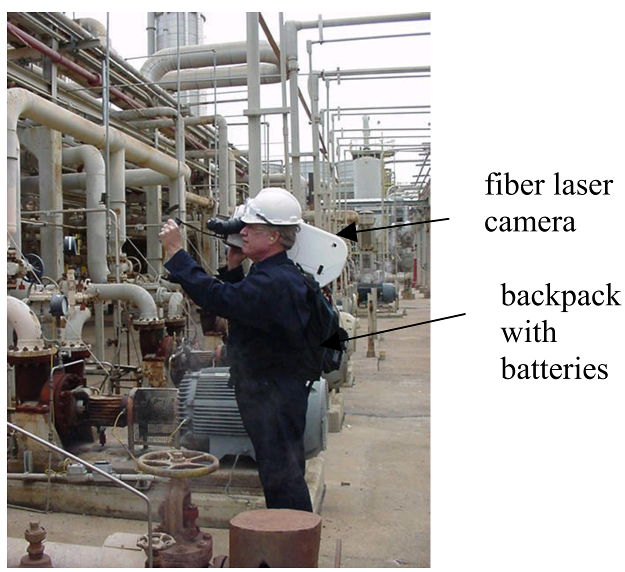

---

[4] SGP – saturated gas plant; USGP – unsaturated gas plant; ISOM – isomerization plant

The results of testing with the CO_2 laser to detect ethylene at two chemical plants are shown in Figure ES 4-4. Bagging analyses showed that the camera detected leaks greater than 1 g/hr. Below 1 g/hr, the laser detected roughly 60 percent of the identified leaks that were bagged.

Figure ES 4-4. CO_2 Laser Performance at Ethylene Facilities During 2002 Testing

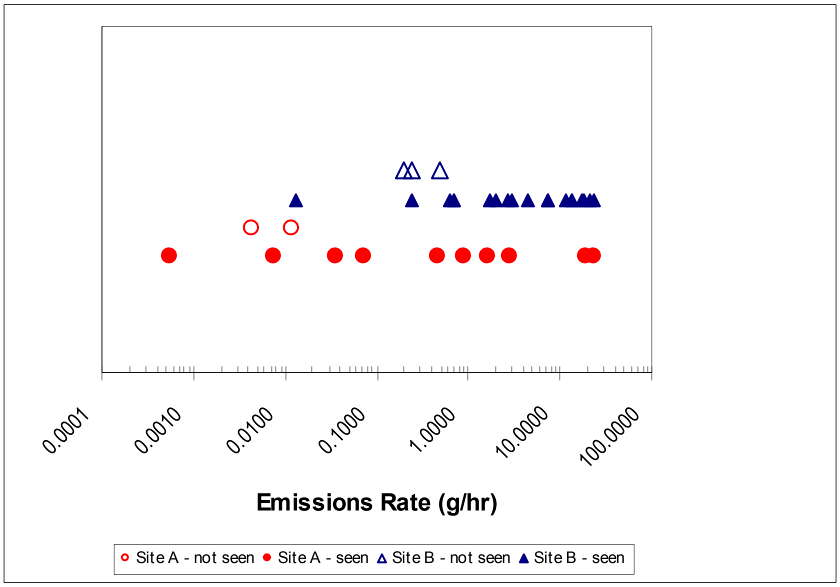

Figure ES 4-5. Scanning an Iced-over Compressor with CO2 Laser at Ethylene Plant

Smart Leak Detection and Repair for Control of Fugitive Emissions

1.0 Introduction

This report presents technology background and test results on an improved Leak Detection and Control method for application in refineries and petrochemical plants. Smart Leak Detection and Repair (LDAR) focuses on locating and repairing the most significant leaking components, cheaper and more quickly than existing LDAR practices. A 1997 study of 11.5 million refinery components showed that over 90% of all-controllable fugitive emissions from refineries are from about 0.1% of all components. This result and statistical analyses show that a Smart LDAR program that focuses on finding and repairing this minority of high "leakers" could result in an improvement in environmental performance. Emerging optical imaging technologies enable adoption of a Smart LDAR program that targets significant leakers. Remote sensing and instantaneous detection capabilities of optical imaging technologies allow an operator to scan process areas containing tens to hundreds of potential leaks. The area being viewed is illuminated with infrared light that allows an image of chemical leaks to be viewed live. Significant leaks are identified immediately, allowing quicker repair, and ensuring efficient use of resources.

This report is organized in two sections:

- Section I - Studies Investigating an Alternative to Current Method 21, and
- Section II – Laboratory and Field Testing of optical imaging technologies

Section I – Studies Investigating an Alternative to Current Method 21

This Section describes studies and analyses undertaken to investigate alternative approaches to existing Leak Detection and Repair (LDAR) programs.

2.0 A Study of Refinery LDAR Data

U.S. refineries are required to implement Leak Detection and Repair (LDAR) programs for processes and streams described in the National Emission Standards for Hazardous Air Pollutants from Petroleum Refineries (40 CFR 63 subpart CC) known commonly as the "Refinery MACT Rule" (MACT is an acronym for Maximum Available Control Technology). The procedures outlined by the current rule are labor and resource intensive, and time consuming.

In 1997, the American Petroleum Institute (API) conducted a study to provide guidance for conducting LDAR programs in a more cost-effective manner. The study evaluated data collected under the LDAR program by 7 Los Angeles, California refineries[5] in the South Coast Air Quality Management District (SCAQMD). The data were examined to help

> **Current LDAR Procedure**
>
> The current LDAR procedure (EPA Reference Method 21) involves placing an instrument probe at the surface of a component seal and measuring the VOC concentration as the probe is moved over the surface of the seal. A correlation has been established relating the mass rate of VOC leaking from the component to the maximum concentration measured by the instrument. EPA and some state agencies have established the level of VOC concentration, which determines a leak. If the concentration is above the level defining such a leak, the component must be repaired or replaced to reduce the concentration to an acceptable level. The leak definition can vary from as low as 100 ppmv to 10,000 ppmv depending on the type of component and the specific regulation.

[5] Screening data were obtained for ARCO, Chevron, Mobil, Shell, Texaco, Ultramar and Unocal refineries.

determine: (1) the design and operational characteristics that influence fugitive emissions and (2) whether a focused LDAR program could be more effective than the current method of monitoring.

2.1 Technical Approach

SCAQMD requires refineries to screen all accessible components (valves, flanges etc.) quarterly and defines a leak at equal to or greater than 1,000 ppmv. The API Study analyzed 11.5 million LDAR program monitoring values collected over 5½ years. Data were analyzed to determine if certain component designs or component applications (e.g. gate valves vs. globe valves, different process units, or different frequencies of actuation) produce more high leakers (i.e. screening ≥ 10,000 ppmv) or more repeat leakers (i.e., screening ≥ 1,000 ppmv more than once in a four-quarter period). Analyses were conducted to find:

- Repeat Leakers –by quarter, for components leaking 2, 3 or 4 times in the preceding four quarters (i.e. chronic leakers) for "leak" definitions of 500, 1,000, 10,000, 50,000 and 100,000 ppmv
- High Leakers – by quarter for components, screening >10,000 ppmv
- Process-by-Process Variations – average for all quarters, comparing repeat (≥ 1,000 ppmv) and high (≥ 10,000 ppmv) leakers for valves, connectors, pumps and an aggregate of all components
- Refinery-by- Refinery Variations
- Mean Time between Failures – a failure was defined as screening >500 ppmv
- Process Unit Comparisons

2.2 Study Results

This study, which is documented in "***Analysis of Refinery Screening Data***" [1], showed that 84 percent of the estimated refinery emissions were from high leakers (>10,000 ppmv), which were only 0.13 percent of the total number of components (Table 2-1 & Figure 2-1)[6]. The average emission rate for these high leakers was approximately 1,000 times higher than the overall average of all components. Of the remaining 16 percent of the estimated emissions, 9.5 percent were from non-leakers (screening <100 ppmv), which constitute 99 percent of the components, and whose estimated emissions are based primarily on an EPA specified, "zero default," value for components that screen at the background concentration. Thus, the high leakers account for about 92 percent of the controllable (i.e., non-default zero) emissions.

[6] The overall percentage of high leakers (screening >10,000) in any of the seven refineries was less than 0.2 percent.

Table 2-1. Distribution of Component Count and Estimated Emissions by Screening Range

Screening Interval ppmv	Total Screening Events	Total Count Distribution %	Emissions lb/hr	Emission Distribution %
0	10,114,633	87.51	19.79	8.34
1-99	1,342,550	11.62	2.63	1.12
100-499	51,894	0.449	2.78	1.18
500 – 999	7,289	0.063	1.04	0.44
1,000 – 9,999	27,198	0.235	11.52	4.91
10,000 – 49,999	8,960	0.078	12.53	5.34
50,000 – 99,999	1,417	0.012	5.37	2.29
≥ 100,000	4,385	0.038	179.01	76.28
Total	**11,558, 326**	**100.00**	**234.67**	**100**

Figure 2-1. Distribution of Component Count and Estimated Emissions by Screening Range

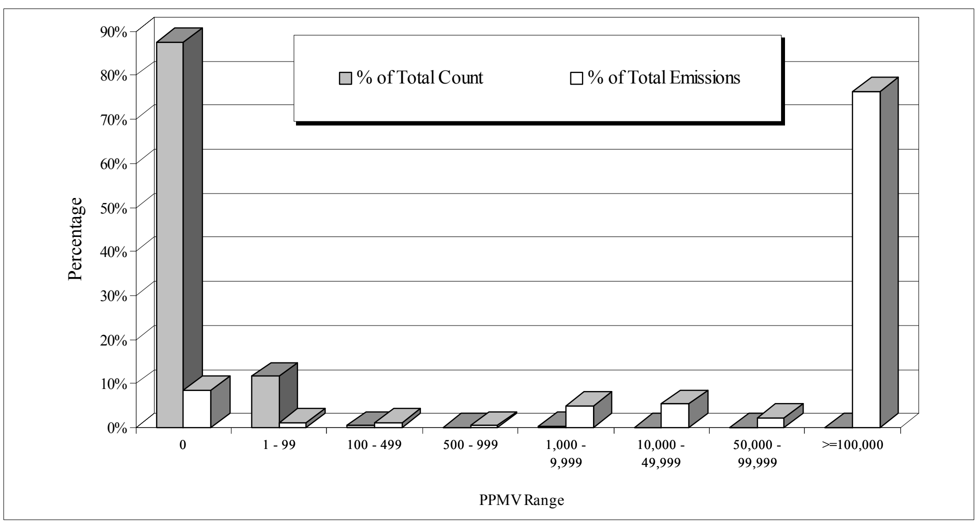

Only 5.4 percent of all emissions were from repeat leakers. The high leakers were found to occur randomly. No systematic explanation for their occurrence was apparent.

Valves accounted for roughly 68% of the total emissions (Table 2-2). Connectors accounted for about a third of total valve emissions even though there were nearly three times more connectors than valves.

Table 2-2. Distribution of Emissions by Type of Component

Component Category	Service	Total Components Screened	Total Emissions for Category, lb./hr	Percent of Total Emissions for Category
Valves	Gas	1.45×10^6	435.70	33.76
Valves	Light Liquid	1.34×10^6	443.20	34.34
Pumps	Light Liquid	3.11×10^6	45.35	3.51
Connectors	Gas	4.54×10^6	221.71	17.18
Connectors	Light Liquid	4.19×10^6	144.75	11.21
	Total	$\mathbf{11.5 \times 10^6}$	**1290.71**	**100.00**

2.3 Study Conclusions

The refinery screening study showed that:

1. About 0.13% of components contribute greater than 90 percent of controllable fugitive emissions;
2. This small population of large leaks are random over time, type of component, and process unit; and
3. Typically, 10,000 components have to be screened to find about 10 significant[7] leaks.

The Study concluded that a more cost effective LDAR program would be one that emphasizes the location and repair of high leakers.

3.0 Optical Imaging Technologies

Two types of optical imagers suitable for detecting hydrocarbon emissions at refineries and chemical plants are:

- A CO_2 laser imager. This is a commercially available instrument, manufactured and marketed by Laser Imaging Systems (LIS) under the brand "Gas Vue®." Gas Vue® utilizes a CO_2 laser. The Gas Vue® was successfully tested at two chemical plants and is referred to as a CO_2 laser imager throughout this report.

- A "fiber" laser imager. This instrument, developed by Sandia National Laboratory's (SNL) Lawrence Livermore facility utilizes a backscatter technique patented by LIS. It is referred to as a "fiber" laser in reference to its optical fiber laser amplifier. It was successfully tested at two refineries and a chemical plant.

Each laser is tuned to emit a specific wavelength of infrared light that provides specific compound or compound type detection. The CO_2 laser is discreetly tunable in the 8-10 micron spectral region. The fiber laser is continuously tunable in the 3 micron spectral region.

Table 3-1 summarizes some of the primary features of the optical imaging units.

[7] High leakers ∃10,000 ppmv.

Table 3-1. Features of the CO_2 – and Fiber Lasers

Features	Fiber Laser	CO_2 Laser
Developer/Manufacturer	Developed by Sandia National Laboratory's Lawrence Livermore facility	Manufactured and marketed under the brand name Gas Vue® by Laser Imaging Systems
Laser Source	Lithium Niobate fiber amplified laser (3-3.5 micron)	CO_2 laser (9-11 micron)
Applicable Refinery and Plant Chemicals	Applicable for aliphatic and olefinic hydrocarbons	Applicable for olefinic hydrocarbons
Testing at Refineries & Chemical Plants	Technology tested at chemical plants and refineries	Technology tested at ethylene facilities
Commercial Availability	Prototype. Discussions regarding commercialization underway.	Available commercially. Used to detect SF_6 leaks at electric power plants

3.1 Backscatter Absorption Gas Imaging (BAGI)

The principle of operation of the CO_2 and fiber lasers is Backscatter Absorption Gas Imaging (BAGI). In BAGI, a video image is produced by illuminating the view area with laser light in the infrared frequency range. The reflected (backscattered) laser light is detected with a camera sensitive to that light. When the chosen laser wavelength is strongly absorbed by the gas of interest, a cloud of that gas is revealed as a dark image. LIS holds a patent for the BAGI principle (U.S. Patent #4,555,627), which is illustrated in Figure 3-1.

Figure 3-1. Schematic Description of BAGI Process

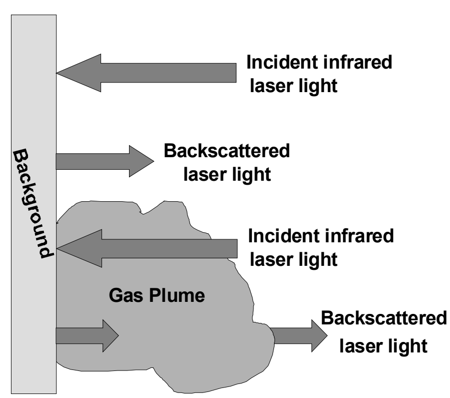

Source: As Adapted from McRae, Tom, *GasVue: A Rapid Leak Location Technology for Large VOC Fugitive Emissions*. (Presentation at the CSI Petroleum Refining Sector Equipment Leaks Group, Washington, DC, Sept. 9, 1997). See U.S. Patent # 4,555,627.

Note: Although this Figure shows the gas in contact with the background material, it is not a requirement that the gas be in contact with the background. The gas plume need only be between the background and the infrared camera.

A video camera-type scanner both sends out the laser beam and picks up the backscattered infrared light. The camera converts this backscattered infrared light to an electronic signal, which is displayed in real-time as a black and white image on both the viewfinder and a video monitor. The same image will be seen whether the scanning is done in daylight or at night because the scanner is only sensitive to illumination coming from the infrared light source, not the sun. The imager can be switched between visible and infrared views; an important attribute when the operator needs to differentiate between steam plumes and gas plumes (see discussion of Atmospheric Window below). Video of the image in the viewfinder can be recorded in both visible and infrared light. Figures 3-2 and 3-3 show leaking components detected by the CO_2 and fiber lasers in visible light and infrared. In their current state of development, these technologies make visible the size of a vapor cloud of certain hydrocarbons and other chemical leaks that are invisible to the naked eye, but they do not yet quantify the mass emission rate of the leak cloud. A detailed technical description of BAGI technology is presented in [3] *"Backscatter Absorption Gas Imaging: a New Technique for Gas Visualization."*

Figure 3-2. CO_2 Laser Views of a Leaking Connector in Visible and Infrared Light

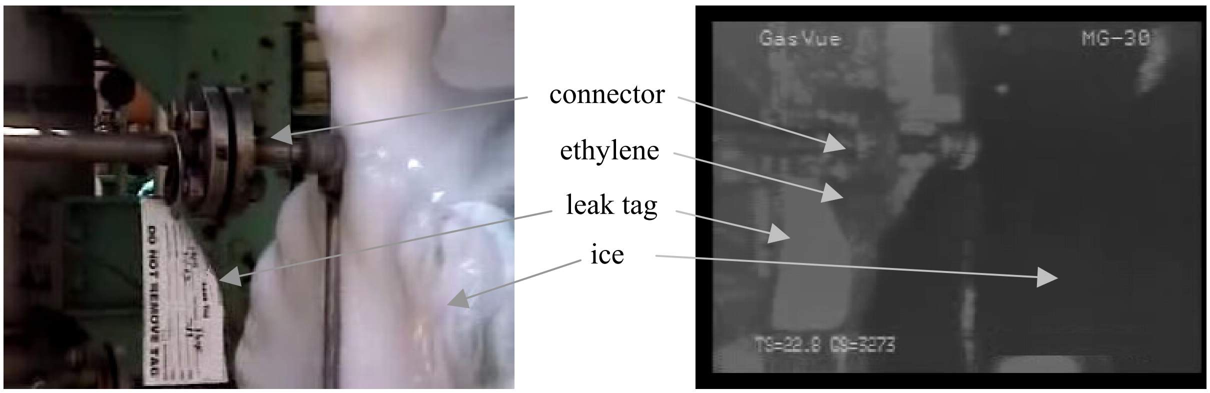

Figure 3-3. Fiber laser Views of a Leaking Flange in Visible and Infrared Light

Visible light view of leaking flange **Infrared view of leaking flange**

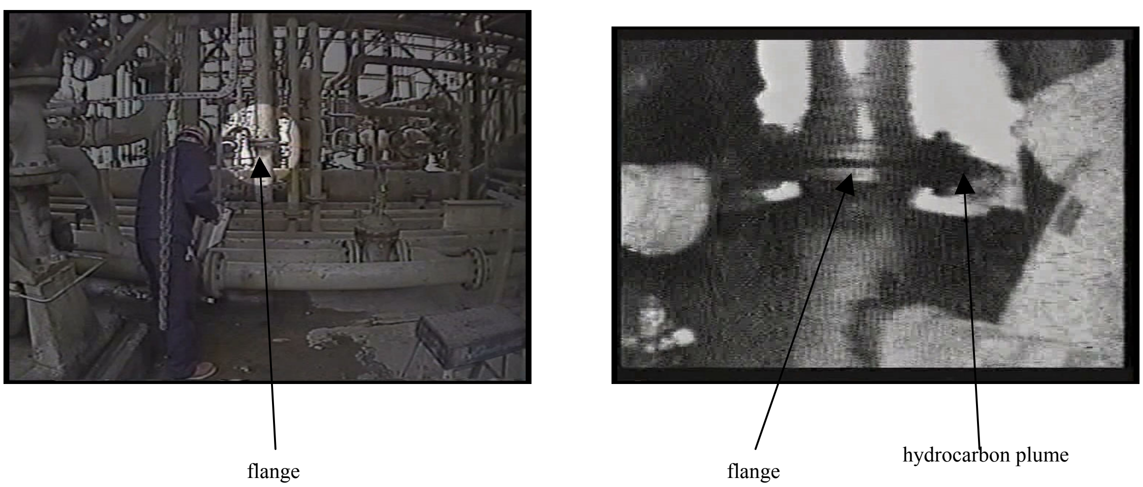

Three parameters that influence the performance of the two BAGI lasers are background, laser wavelength and atmospheric window.

Background. For the technology to observe a leak, there must be a reflective, or backscattering, surface behind the leak. It is not possible to visualize a gas plume against the sky or a distant background. It is possible in many circumstances to image a leak against the component itself, with a distant or sky background appearing black. The operator knows that the imager is beyond detection range when the camera no longer produces an image of the components under inspection: the more distant the component or background, the darker the image. The operator can also switch the camera between infrared and visible light viewing to determine whether there is an adequate background surface behind the leak point being inspected.

Laser Wavelength. Gas leak detection sensitivity by optical imaging depends strongly on the match between the laser wavelength and the wavelengths of absorption by the gas of interest. To produce an image in the viewfinder of a black cloud where the hydrocarbon gas is present, the gas cloud must be capable of absorbing the laser wavelength.

Wind speed, optical resolution, gas plume motion and viewing angle also affect detection sensitivity. The higher the wind speed, the more quickly the gas is dispersed as it leaves the leak source, and the less visible it becomes to the optical imager. However, some motion is beneficial for detecting a leak, as the human eye is particularly sensitive to movement of the gas plume. A stationary gas cloud is very difficult to distinguish against a non-uniform background.

Atmospheric Window. An "atmospheric window" is defined as a region of the spectrum where there is minimal or no light absorption by oxygen, nitrogen, carbon dioxide, and water vapor that are normally present in air. The major atmospheric windows in the infrared region are found in the 3 to 4.2 micron and in the 8 to 13 micron wavelength regions. A laser beam propagating through the atmosphere at wavelengths within these atmospheric windows will experience minimal attenuation.

However, laser light within these IR windows may still be attenuated by particulates in the air, including water droplets as in fog and steam. Consequently, these particulates will appear as dark clouds in the BAGI image as do the fugitive gases that absorb the laser light. However, since these particulates are also visible to the naked eye (while the fugitive gases are not), the BAGI operator can easily distinguish between the two types of cloud displays.

For example, if the cloud can be seen with the unaided eye AND with the BAGI camera – the cloud is likely particulates or steam. If the cloud can only be seen with the BAGI camera, it is hydrocarbon vapor.

3.2 Description and Operations of the CO_2 and Fiber Lasers

The CO_2 and fiber lasers, which each weigh between 9 kg and 14 kg and are about the size of a TV camera, consist of two systems: a camera unit and a power/control unit. The camera portion of the CO_2 laser is connected to a mobile power pack that plugs into an external 110V AC outlet. The power pack converts AC to DC. The camera portion of Sandia National Lab's prototype fiber laser plugs into a backpack borne power/control that is powered by a 28V lithium-ion battery. Battery lifetime while the fiber laser is operational is between 1 and 1½ hrs; batteries recharge in twelve hours. Batteries can be changed without shutting down the device. SNL's Imager can also be operated on a 110 volt AC outlet through the power unit's 28-volt DC converter.

Both laser cameras can be operated in a shoulder-mounted position or with a tripod-mounted position (Figure 3-4). The tripod has a swivel fitting that permits the operator to move the instrument from left to right and up and down while scanning for leaks. A zoom lens allows the operator to adjust the focal distance to obtain a better view. The operator can switch between the infrared view and visible light, and can record video of the image seen in the viewfinder in both views. Both cameras have simple start up procedures requiring 10 – 15 minutes after power is switched on.

Figure 3-4. Laser Imagers shown Shoulder- and Tripod-Mounted Operations

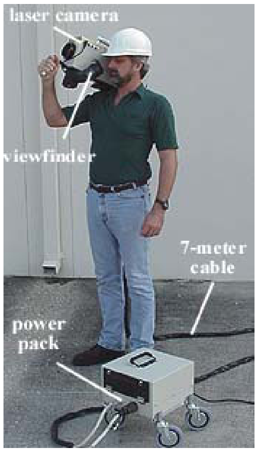

CO_2 Laser

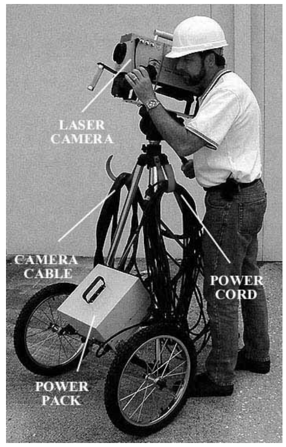

CO_2 Laser

Fiber laser

3.2.1 Description of the CO_2 Laser Components

The CO_2 wave guided laser operates in the 9-11 micron spectral region at 5W. Use of such a low laser power is possible due to the unique optical arrangement shown in Figure 3-5, which permits synchronous scanning of a laser beam and the instantaneous field-of-view (IFOV) of an infrared detector across the area of interest. The IFOV produced by the small (.005 cm X .005 cm), cooled IR detector and a collimating lens is scanned in a raster-like fashion across the target area by two scan mirrors, one for horizontal motion and another for vertical motion (in the same fashion as a television picture tube). The laser beam is directed onto, and scanned across the target area by these same two scan mirrors. This insures that the detector IFOV and the laser beam are in perfect synchronization, and that the laser only need irradiate that region of the target area viewed by the detector. In these long-range systems (>10 m), a beam expander is used to reduce the laser beam divergence so that it is less than the IFOV divergence. This keeps the laser power requirements to a minimum.

See *"Evaluation of the GRI Gas Imaging Leak Survey System,"* [4], and *"GasVue VOC and SF6 Leak Location Field Test Results,"* [5] for additional details about the CO_2 laser.

Figure 3-5. CO_2 Laser's Synchro-Scan Optical Configuration

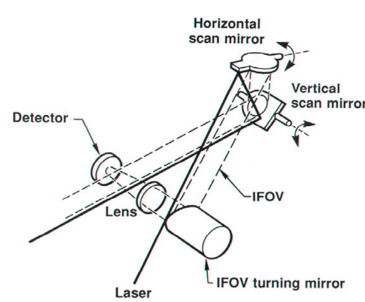

3.2.2. Description of Sandia National Laboratory's Fiber Laser

Sandia National Laboratories (SNL) developed an infrared laser source that is effective for VOC emissions at industrial facilities. The device is an optical parametric oscillator (OPO), which uses a crystal of periodically-poled lithium niobate (PPLN) as its active medium. An OPO is a laser-like device that consists of an optical cavity, which contains a nonlinear crystal (i.e., the PPLN). To operate the OPO, a beam from a separate laser (the pump laser) is focused into the PPLN crystal. Light from the pump laser is converted by the OPO into two new beams (called the signal and idler) whose frequencies add to that of the pump laser. The basic elements of the PPLN-based imager are shown in Figure 3-6. They consist of the pump laser, the OPO, and the raster scanner.

Figure 3-6. The basic elements of the PPLN-based imager

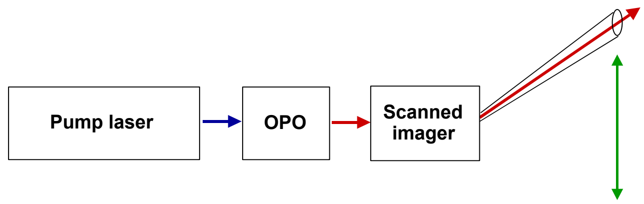

(1) The pump laser creates the initial laser radiation

(2) The OPO converts the pump light to the infrared

(3) The scanned imager creates the laser-illuminated image

The current prototype SNL fiber laser was preceded by several generations including a van-mounted and table-mounted miniature version.

4.0 Determining Equivalent Leak Definitions for Alternative Work Practices to Method 21

Current U.S. EPA regulations governing control of fugitive emissions do not permit the use of optical imagers or the Smart LDAR concept. However, a provision in U.S. EPA's regulations allows stakeholders to petition the Agency to recognize/permit alternative controls or work practices that will provide equal or better environmental protection to the specific current requirements[8]. Because field demonstration and testing of potential new fugitive emissions control technology or work practices are potentially quite costly, U.S. EPA has developed a demonstration protocol. This demonstration protocol provides an "approval process" that includes a combination of laboratory testing, field testing and mathematical analysis to quantify the performance of an alternative technology and determine if it can achieve equivalent fugitive emissions control to that achieved using Method 21 monitoring.

To facilitate this demonstration of emissions control equivalence for a new technology, the U.S. EPA has developed a Monte Carlo simulation SAS®-based software to help evaluate technologies or work practices that may be proposed as alternatives for use in LDAR programs. The software performs Monte Carlo simulations (i.e., random statistical simulations) of simultaneous equipment screenings by the current work practice that use Method 21 and by a proposed alternative control technology. Predicted emission reductions are calculated for equipment components identified as leakers to quantify the environmental benefit derived from using either the existing or new technologies in a LDAR program. Environmental benefit equivalent to the current work practice (i.e. Method 21) is demonstrated when Monte Carlo simulations show that emission reduction for an alternative technology is the same as, or larger than, the current work practice emission reduction.

[8] Washington DC, United States Environmental Protection Agency, Code of Federal Regulations 1990b: Title 40, Part 60 Subpart GGG, "Standards of Performance for Equipment Leaks of VOC in Petroleum Refineries," Government Printing Office.

API undertook a Monte Carlo Analysis for valves to determine a leak definition for an Alternative Work Practice (e.g. optical imaging) that would result in equivalent environmental protection as Method 21 monitoring.

Monte Carlo Analysis Focused on Mass Equivalent

Current LDAR monitoring technologies provide a screening value in ppmv. However, field bagging studies have shown that components with high ppmv screening values may have low mass leak rates. A "Smart" LDAR approach, would emphasize large leakers in mass, hence the Monte Carlo analysis focused on determining a leak in rate in mass (Kg/hr) that would be equivalent to the control achieved by current ppmv leak definitions.

For each Method 21 leak definition in ppmv, the Monte Carlo analysis developed an equivalent leak definition in mass rate for the Alternative Work Practice (AWP). Because Smart LDAR is independent of monitoring technology, the AWP equivalent mass leak rates are applicable to any technologies, including optical imaging devices, that are used instead of current (Method 21) LDAR monitoring practices.

Summaries of the technical approach, results and conclusions are presented below. Detailed discussions are presented in "*Equivalent Leak Levels & Monitoring Frequencies for Smart LDAR*" [6].

4.1 Technical Approach to Monte Carlo Simulations

One thousand simulations were performed using actual valve fugitive emissions data from an "uncontrolled" plant for each combination of optical imaging and Method 21 leak definitions and monitoring frequencies. Five monitoring frequencies were simulated for evaluating the control effectiveness of optical imaging technology:

- Quarterly (once per quarter)
- Bi-monthly (once every two months)
- Semi-Quarterly (twice per quarter)
- Monthly (three times per quarter)
- Semi-Monthly (six times per quarter)

The study determined equivalent mass leak rate definitions (g/hr) for optical imaging (or other AWP) using these monitoring frequencies and achieving equivalent emissions control for three typical Method 21 leak definitions used in the established state and federal regulatory LDAR programs that require quarterly monitoring:

- 500 ppmv
- 1,000 ppmv
- 10,000 ppmv

The underlying basis used in the Monte Carlo approach is the comparison of emission reductions resulting from screenings by the two leak detection methods. The benchmark against which the optical imaging method (or AWP) is evaluated is the emission reduction achieved by the currently required method, U.S. EPA Reference Method 21.

4.2 Results and Conclusions

The Monte Carlo analyses found that the mass emission rate for a given optical imaging or other AWP monitoring frequency, equivalent to a specified Method 21 leak definition, was fairly precise and unambiguous.

The study showed that, for valves, optical imaging (or other AWP), used at bi-monthly monitoring frequency, provides greater environmental protection than the current Method 21 quarterly monitoring for leak definitions of 500 ppmv, 1,000 ppmv, and 10,000 ppmv. Table 4-1 shows the equivalent AWP leak definitions at the five different monitoring frequencies for three CWP leak definitions at quarterly monitoring.

Table 4-1. AWP Leak Definitions at Different Monitoring Frequencies for Valves Equivalent to Three Method 21 Leak Definitions at Quarterly Monitoring

Method 21 Leak Definition at Quarterly Monitoring	Equivalent AWP Leak Definition for Specified Monitoring				
	Quarterly (once per quarter)	Bi-Monthly (once every 2 months)	Semi Quarterly (twice per quarter)	Monthly (thrice per quarter)	Semi-Monthly (six times per quarter)
500 ppmv	0.00023kg/hr	0.060 kg/hr	0.085kg/hr	0.10 kg/hr	0.17 kg/hr
1,000 ppmv	0.00041 kg/hr	0.061 kg/hr	0.085 kg/hr	0.11 kg/hr	0.17 kg/hr
10,000 ppmv	0.0049 kg/hr	0.069 kg/hr	0.090 kg/hr	0.13 kg/hr	0.18 kg/hr

5.0 Alternative Work Practice and Smart LDAR overcome Variability in Method 21

Equivalent total emissions reductions when using the proposed AWP are achieved by identifying all of the highest rate leakers. This is illustrated in Figures 5-1 and 5-2.

Figure 5-1 shows that the data supporting the correlation of screening values with the mass emission rate is highly scattered. The screening value is characteristic of the leak rate as a concentration (ppmv) but the mass rate (kg/hr) is a direct measure of the leak. There is much variability between the Method 21 screening rate and the measured mass emission rate. As shown in Figure 5-1, for any mass emission rate the Method 21 screening value can range over several orders of magnitude. There is the likelihood, therefore, of both false positives and false negatives when using Method 21 to find leaking components.

False positive Method 21 measurements result in added and unnecessary effort to repair components that, although indicated by Method 21 to be above the leak definition, have mass emission rates that are below this equivalent value. There are very little if any emission credits for these repairs.

False negatives from Method 21 can result in significant emissions because, although not indicated by Method 21 screening measurement, the equivalent mass emission rate is above the definition where repair is required. These components would not be repaired and would continue to leak under a Method 21 based program. Since these components would be identified as leakers by the optical imaging (or AWP), the reduction of these emissions, which were "missed" by Method 21, is a major advantage for using the optical imaging technology. Thus, the new Smart LDAR approach using optical imaging allows a much higher mass leak definition than when using Method 21 since missed leaks are found and repaired.

Figure 5-1: Variability of Method 21 Results for Equivalent Mass Emission Rates

Note: In a box plot, boxes enclose the middle half of the data spread, from the 25th to the 75th percentiles, with a horizontal line drawn inside the box at the median (50th percentile) value; vertical lines (whiskers) extend below the box to the 5th percentile value and above the box to the 95th percentile value; and "dots" indicate values smaller than the 5th percentile value or larger than the 95th percentile value.
Source: *Monte Carlo Simulation Evaluation of Gas Imaging Technology*

This illustration shows box plots for 1993-94 Petroleum Industry bagging dataset (American Petroleum Institute, 1993a; 1993b; and 1994) depicting reported screening value ranges (ppmv) for different "levels" of mass emission rates, denoted by mass magnitude bins (e.g., mass emission rate magnitude "1E-8" indicates mass emission rates with units of 10^{-8} kg/hr; i.e., values 1H10^{-9} kg/hr or larger, and less than 1H10^{-8} kg/hr, because the integer portion of the base-10 logarithm for values between these bounds is "-8").

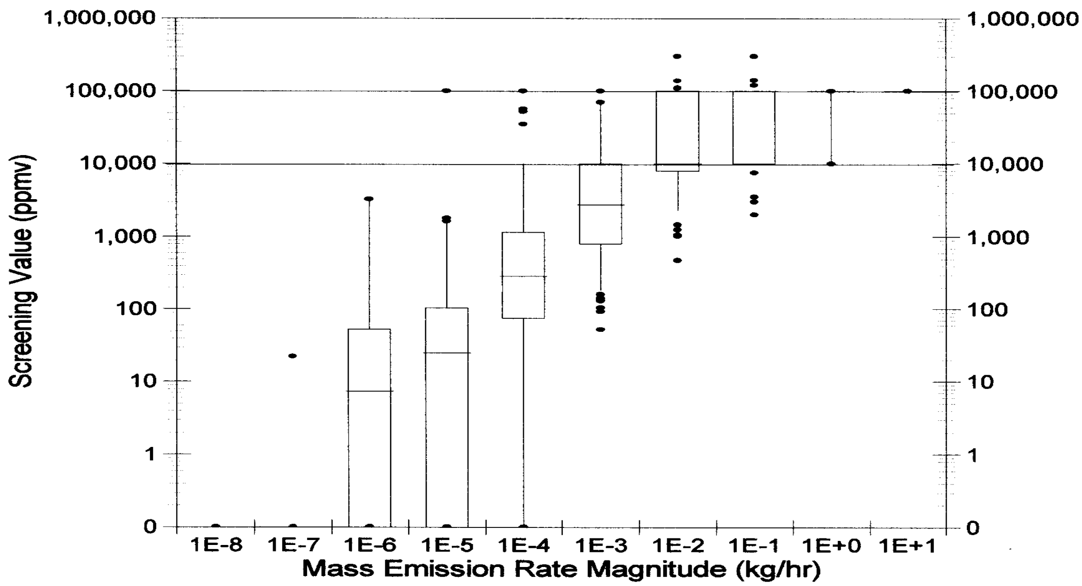

In the current fugitive emission control program required by U.S.EPA regulation, monthly or quarterly monitoring is required with a leak definition for repair of 500, 1,000 or 10,000 ppmv. Less frequent monitoring is allowed if the percent of leaking components remains below a specified level for a specified number of periods. In some U.S. state regulations, the leak definition is even lower, which is in direct contradiction with the results of the API study shown in Figure 2-1. Lower leak definitions for repair do not necessarily lead to better emissions control since, as the leak level is decreased, few additional leaking components are added to the repair group and these contribute very little to the overall mass emissions.

The Smart LDAR approach, as illustrated in Figure 5-2, focuses on identifying and repairing the highest leakers since these are the source of almost all the mass emissions. Equivalence is obtained by more quickly finding and repairing these large leaks, which more than off-sets the emission rates from components with low ppmv readings that leak for longer periods. The use of optical imaging could provide a more cost effective approach to more quickly find the high leakers. This, combined with the potential to find the false negatives (missed high leakers) from the Method 21 approach, results in the potential large emissions control benefits from the Smart LDAR technique using the optical imaging technology.

Figure 5-2. Equivalence From Quicker Repair of Highest Leakers

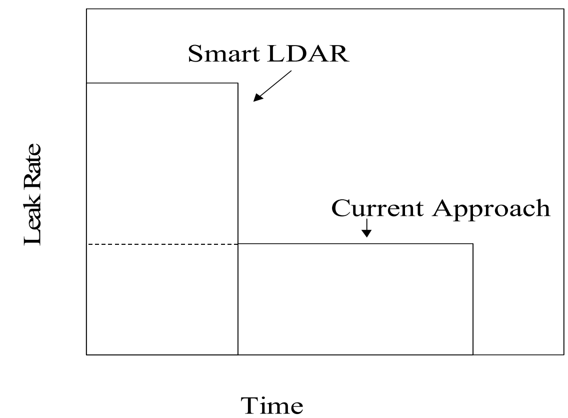

Note: Not drawn to scale. This diagram illustrates the concept that Smart LDAR (on average) finds large leaks in shorter time, which are equivalent to the smaller leaks over longer time. The total reduction is equal under both approaches, but more cost-effective under Smart LDAR.

Section II – Laboratory and Field Testing of Optical Imaging Technologies

A number of studies have been conducted to characterize the performance of the CO_2 and fiber lasers in detecting fugitive emissions. These include two studies at refineries, two at ethylene production plants, and two under controlled laboratory conditions. There have been several additional demonstrations. This section summarizes the objectives and outcomes of these laboratory and field tests.

6.0 Refinery Demonstration of a Van-Mounted Fiber Laser

In April 1999, U.S. EPA, API, Sandia National Laboratory (SNL), and Laser Imaging Systems (LIS) conducted a demonstration of a van-mounted prototype of the fiber laser developed by LIS and SNL. The objectives of the four-day demonstration, which took place at a Texas refinery, were to:

- Demonstrate that the fiber laser could work reliably for an extended period of time in a refinery setting, and
- Determine whether this technology performed well enough compared with existing Method 21 devices to warrant continued development.

6.1 Methodology

Two teams, working independently, collected data from seven process areas (see Text Box).

- **The Method 21 Team** primarily monitored tagged components subject to current LDAR programs.

The population of components selected for Method 21 monitoring was defined by two parameters:

1. Components had to be within reach of the OVA operator standing on the ground, and
2. Components had to be within the line-of-sight and range of the minivan carrying the fiber laser.

This meant that a relatively small fraction of the total number of components at each of the seven process areas was monitored. The Team also noted the time required to complete the monitoring.

Process Areas Monitored

- Aromatics Unit
- Catalytic Cracking Unit
- Crude Distillation Unit
- Hydrocracker Unit
- Product Piping Manifold
- Pipe Rack
- Propone Storage

- **The Fiber Laser Team** monitored all components within the laser's line of sight and distance of image detection. All leaks found by the Fiber Laser Team were immediately quantified (in ppmv) using a TVA detector and assigned an identification number if not already tagged. Given the nature of the technology, the fiber laser can detect leaks from all sources in its line of sight irrespective of whether the component is subject to the specific LDAR regulatory requirements for monitoring. Therefore, the number of components that were monitored by the fiber laser included all components monitored by the Method 21 Team plus all other components in the line-of-sight and range of the unit. The Coordination Team (responsible for overall design and management of the demonstration) estimated the number of components that the Fiber Laser Team monitored. Both infrared-light and visible-light video of all areas monitored were recorded.

6.2 Findings & Conclusions

The demonstration showed that the van-mounted fiber laser could successfully detect fugitive emissions.

The Test Team reached three conclusions from analysis of the collected data:

- The fiber laser could be used to locate high leaking components in a refinery setting.
- The majority of VOC mass emissions at a refinery come from a small percentage of components with large leaks, and optical imaging has the potential to more efficiently identify those leaking components.
- The demonstration results justified continued development of an operator-portable prototype of the fiber laser.

7.0 Laboratory Testing of Primary Components of an Operator-Portable Fiber Laser

In 2000, Sandia National Laboratories (SNL) conducted a lab test of the unassembled elements of an operator-portable fiber laser. The test instrument consisted of the OPO from the van-mounted fiber laser coupled to a new scanner designed by LIS.

The test goal was to evaluate the influence of leak source, viewing distance, wind speed, reflective background, effluent gas, and mass flow rate on the leak detection threshold of the fiber laser under lab conditions.

7.1 Test Methodology

The leak originated from a valve assembly that sat inside a wind tunnel during the test. The fiber laser was placed on a cart in front of the wind tunnel view port such that the operator had a direct sight line to the generated plumes. Images of the view through the viewfinder were recorded on videotape.

The test parameters and matrix are shown in Tables 7-1 and 7-2, respectively.

Table 7-1. Laboratory Test Operational Parameters

Parameter	Baseline value
Leak source	Threaded plug
Viewing Distance (m)	3
Effluent gas	Propane
Wind speed (meters/s)	1
Background material	Sandpaper
Mass flow rate[1]	0.2*LDL to 5*LDL, continuously varied

m = meters
LDL = lower detection limit

A run was conducted by increasing the mass flow until the plume became visible. Video was collected continuously for a range of mass flows ranging between one-fifth of the lower detection limit (0.2*LDL) and five-times the lower detection limit (5*LDL), where the lower detection limit determined by the operators at the time of recording.

Table 7-2. Operator-Portable Fiber Laser Laboratory Test Matrix

Test	Leak Source	Viewing Distance (meters)	Effluent Gas	Wind speed (meters/s)	Background material
Baseline	Plug	3	Propane	1	Sandpaper
1	Bonnet	3	Propane	1	Sandpaper
2	Flange	3	Propane	1	Sandpaper
3	Plug	6.1	Propane	1	Sandpaper
4	Plug	9.1	Propane	1	Sandpaper
5	Plug	3	Propane	1	Sandpaper
6	Plug	3	Propane	1	Sandpaper
7	Plug	3	Propane	1	Sandpaper
8	Plug	3	Propane	1	Sandpaper
9	Plug	3	Propane	5	Sandpaper
10	Plug	3	Propane	10	Sandpaper
11	Plug	3	Propane	1	Styrofoam
12	Plug	3	Propane	1	None

Fifteen repetitions were done of the baseline tests and 6 repetitions for the tests that varied the other parameters. For each repetition, a segment of videotape was recorded in which the gas flow was continuously varied from a value of 0.2*LDL to 5*LDL. A panel of five observers, familiar with gas imaging video, reviewed the data. Each observer viewed a third of the video segments – i.e., 5 segments for the baseline runs and 2 segments for the parameter variation runs. The mass flow rate at which the flow became visible for each observer was recorded. Values of all runs and observers were used to generate mean leak detection levels (LDL) and a measure of their variability.

7.3 Test Results and Analysis

For a given test condition, the gas flow was initially adjusted to find the lowest detectable level (LDL), as it appeared to the test operators. Following this, an attempt was made to record imagery at mass flow rates spanning the range between 0.2*LDL and 5*LDL. The recorded data were assessed in two different ways:

- First, a single observer viewed the tapes and determined the point at which the visibility threshold occurred.
- Second, a panel of observers viewed the data and indicated the intensity of leak that was observed (if any).

A brief discussion of the primary results is presented below. Past experience indicates that the detection limit may be higher when viewing tapes as compared to viewing through the instrument in real time.

7.3.1 Single Observer Results

The single-observer results are summarized in Table 7-3. The LDL values are shown as a mass flow (grams per hour, g/hr) and the corresponding screening value (SV, ppmv) (determined using EPA correlation equations). The flange correlation equation was used for the bonnet and flange leak.

The mass flow LDL values are listed in two ways— the LDL viewed at the leak point and that viewed in the downstream plume area. The LDLs are larger in windy downstream area because the wind rapidly dissipated plume in this area. The leak point thresholds are slightly lower because wind affects the gas less at this location. In general, the detection limits were between 2.2 and 3 g/hr for a wind speed at 1 meter per second (m/s) at all viewing distances against sandpaper.

Wind speed had the most effect on the single observer results. The LDL values observed at both the leak point and in the plume area increased considerably, when all other baseline conditions were held constant and wind speed increased from 2.5 m/s to 10 m/s.

Background also influenced results. Against a Styrofoam background, with all other baseline conditions held constant the, LDL increased to 6 g/hr. In this case, the laser return was so bright that it overwhelmed the camera and the laser power had to be reduced to 20-60 mW.

Table 7-3. Leak Detection Thresholds

Test	Leak Point	Range (meters)	Gas	Wind Speed (meters/s)	Background Material	LDL (grams/hr) at Leak Point	LDL (grams/hr) in Plume Area	Approx. SV*** (ppmv)
Baseline	Bonnet	3	Propane	1	Sandpaper*	2.8	Same	9,100
1	Threaded Plug	3	Propane	1	Sandpaper*	2.2	Same	---
2	Flange	3	Propane	1	Sandpaper*	2.5	Same	7,750
3	Bonnet	6.1	Propane	1	Sandpaper*	3.0	Same	10,050
3b	Bonnet	7.6	Propane	1	Sandpaper*	3.0	Same	10,050
4	Bonnet	9.1	Propane	1	Sandpaper*	3.0	Same	10,050
9a	Bonnet	3	Propane	2.5	Sandpaper*	3.0	4.0	10,050
9	Bonnet	3	Propane	5	Sandpaper*	7.5	10.0	37,000
9b	Bonnet	3	Propane	7.5	Sandpaper*	13.0	18.0	80,900
10	Bonnet	3	Propane	10	Sandpaper*	27.0	35.0	228,750
11	Bonnet	3	Propane	1	Styrofoam**	6.1	Same	27,550

Laser power: 500 mW** * Laser power: 20 to 60 mW** ***** Screening Value**

7.3.2 Panel of Observers Results

In the "panel of observers" test, the data were assessed using a panel of five viewers. Their familiarity with gas imaging ranged from none to very familiar. Each panelist was initially "trained" by allowing them to view imagery of a nonleaker, a borderline leaker, and a high leaker. The panelists were then shown a tape containing image segments collected at a given range. The segments were dubbed onto this tape in random order with respect to gas flow rate, background material, and leak location. For each segment, the viewer was asked to grade the intensity of the leak observed from none to low, medium, or high (0, 1, 2,3). The reviewed segments were a subset of the total dataset collected. They consisted of the highest leak, the lowest leak, and four near the apparent transition region.

The lowest flow rates visible to the panel of viewers are listed in Table 7-5. The corresponding test conditions and the number of observers who detected the leak are presented.

Table 7-5. Lowest Leak Detection Thresholds Detected by Panel of Observers

Viewing Distance (meters)	Wind Speed (meter/s)	Background Material	Lowest Detected Flow at Leak Point (grams/hr)	Leak Position	Number of Panelist who could See Leak
3	1	Sandpaper	0.8	Threaded plug	1 of 5
3	2.5	Sandpaper	1.5	Bonnet	4 of 5
3	5	Sandpaper	3.5	Bonnet	5 of 5
3	7.5	Sandpaper	3.1	Bonnet	4 of 5
3	10	Sandpaper	8.9	Bonnet	4 of 5
6.1	1.2	Sandpaper	1.5	Bonnet	5 of 5
3	1	Sandpaper	1.5	Bonnet	5 of 5
3	1	Styrofoam	4.9	Bonnet	5 of 5

The panel results differed from the individual observer results in some cases. The video collected at 1 m/s wind speed is relatively similar (visibility onset of ~2-3 g/hr in each case for sandpaper; 4.8 vs. 6 for styrofoam). At higher wind speeds, however, the two values begin to diverge, with the panel results producing a lower detection threshold than the single observer. For example, at 2.5 m/s, the results are 1.5 g/hr for the panel and ~3 for the individual; and at 7.5 m/s they are 3 g/hr vs. 13 g/hr. The discrepancy between the panel and individual is believed due to the single observer being more conservative in defining the threshold at a level that was obviously visible (i.e., ranking high on the panels scale). In contrast, the panels were told to focus on all leaks and to rank their intensity.

8.0 Laboratory Tests of SNL's Portable Fiber Laser

In 2001/2002, Sandia National Laboratory conducted tests of its prototype portable fiber laser at its Lawrence Livermore facility. The objectives of the laboratory tests were to:

- Develop data to establish a relationship between operating variables (e.g. operator influence, mass leak rate, wind speed, type of reflective background, reflectivity of background, and viewing distance from the leak) that can be used to define the performance of the portable fiber laser.

- Determine whether, within a controlled environment using simulated industrial components, the prototype fiber laser BAGI system can detect hydrocarbon leaks of a mass rate equal to the equivalent leak definition values for an alternative work practice as determined by the Monte Carlo analysis.

- Gather sufficient data and develop a statistical correlation of the operating variables with the leak detection threshold, which could allow EPA-OAQPS to prepare alternative work practice guidelines that permit the use of optical imaging technology for the Leak Detection and Repair (LDAR) program.

8.1 Test Methodology

Propane was used as the leak gas in the test, which was conducted in two phases:

- Phase 1 -- A controlled test in which the leaking component was placed in a wind tunnel to control windspeed and the imager was mounted on a cart positioned to allow it to view the component. For a given distance, windspeed and reflective background, the mass rate detection threshold was determined. The test results were used to develop a correlation of the mass rate detection threshold with wind speed, viewing distance, and background reflectivity. Table 8-1 shows the test variables.

Table 8-1. Wind Tunnel Test Variables

Viewing Distance (meters)	Windspeed (meters/s)	Backgrounds
3	Near 0	Sandpaper
6.1	1	Curved metal (painted)
9.1	10.8	No background*
*The component itself acts as the reflective background.		

- Phase 2 -- referred to as "The Roving Test" was conducted outdoors. Four leak stations with different test components were erected in different positions and with different backgrounds. A system operator carried the imager to view the components. The test was conducted in a "blind" fashion where the system operator had no knowledge of which component was leaking. The test was repeated under different conditions, as the component that was leaking was varied.

The roving test utilized the results from the wind tunnel testing. The Test Team monitored wind speed to determine when it was in the range between 0 and 10 meters/s (the range tested in the wind tunnel). When the appropriate wind conditions were met, a test was set up. The expected mass detection threshold for the observed wind speed and a given range (3 or 6.1 meters) was presumed to be equal to that observed in the Phase I wind tunnel tests. Then, a leak of this mass rate was started at one of the four test stations. For example, if the average wind speed of 1.5 m/s was observed on a given test day, consultation of the Phase I data would show that the expected mass detection threshold would be 5 g/hr at a range of 3 m. Thus, a leak of 5 g/hr was set up at one of the test stations in the roving tests.

The laser operator did not know which station was leaking. Starting at 9.1 m viewing distance, the operator attempted to detect the leak. The operator continued moving closer to the leak stations until he verbally indicated that he saw the leak and correctly identified the leak station. If he indicated that he saw the leak, but identified the wrong station (which is possible if a wind is blowing the leak plume), the Test Team noted this as a false positive and told the operator to keep searching until he identified the correct leak station. Once the operator correctly identified the leaking component, the threshold viewing distance for that mass threshold and the wind speed were recorded. Table 8-2 describes the roving test stations. Figures 8-1 and 8-2 show an illustration and a photo of the Roving Test set up.

Table 8-2. Roving Test Stations

Station	Description of Roving Test Stations
Station 1	Component mounted at eye level (1.2 meters) with sandpaper background
Station 2	Component mounted at eye level (1.2 meters) with painted curved sheet metal background (primed and painted with Rust-O-leum flat grey spray paint)
Station 3	Component 0.51 meters above the ground, no background. At this height, the pavement under the component can serve as a background in a similar way as a concrete pad or a paved refinery process area would serve as a background
Station 4	Component 2 meters off of the ground with open sky in the background. Since Station 4 is above eye level, the component itself is the reflecting background.

Figure 8-1. Roving Test Set-up

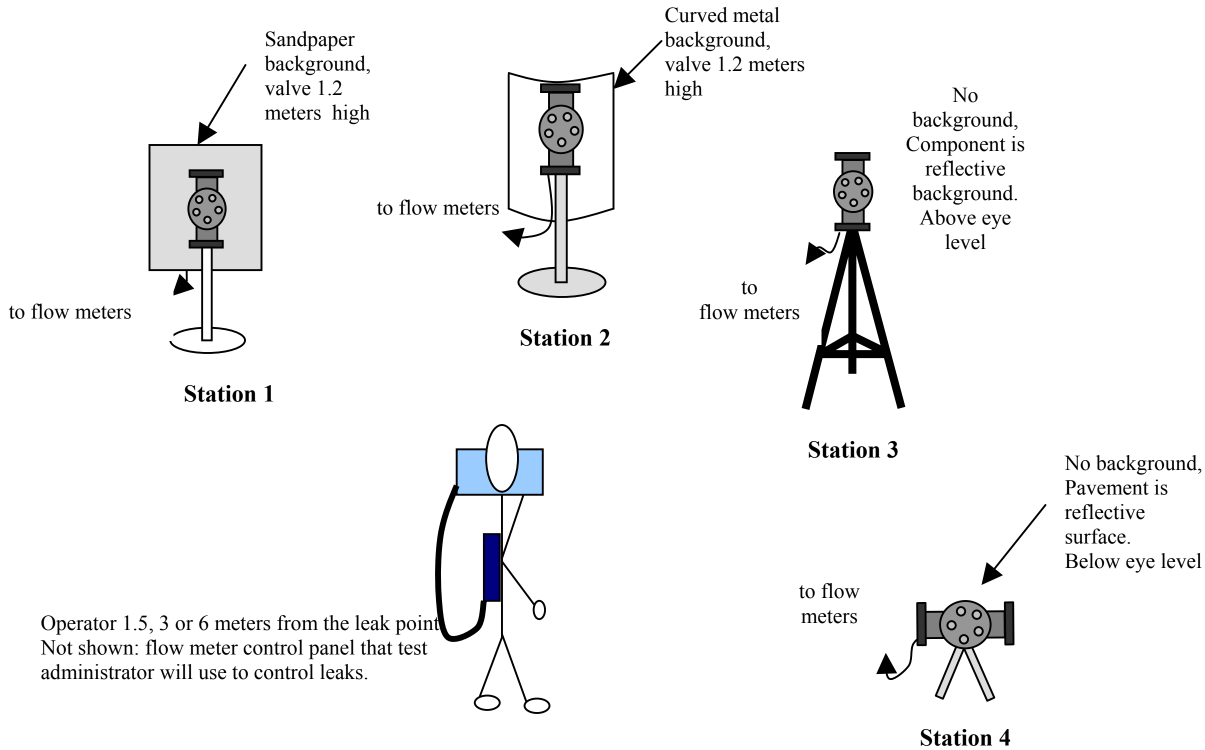

Figure 8-2. Test Stations for Roving Test

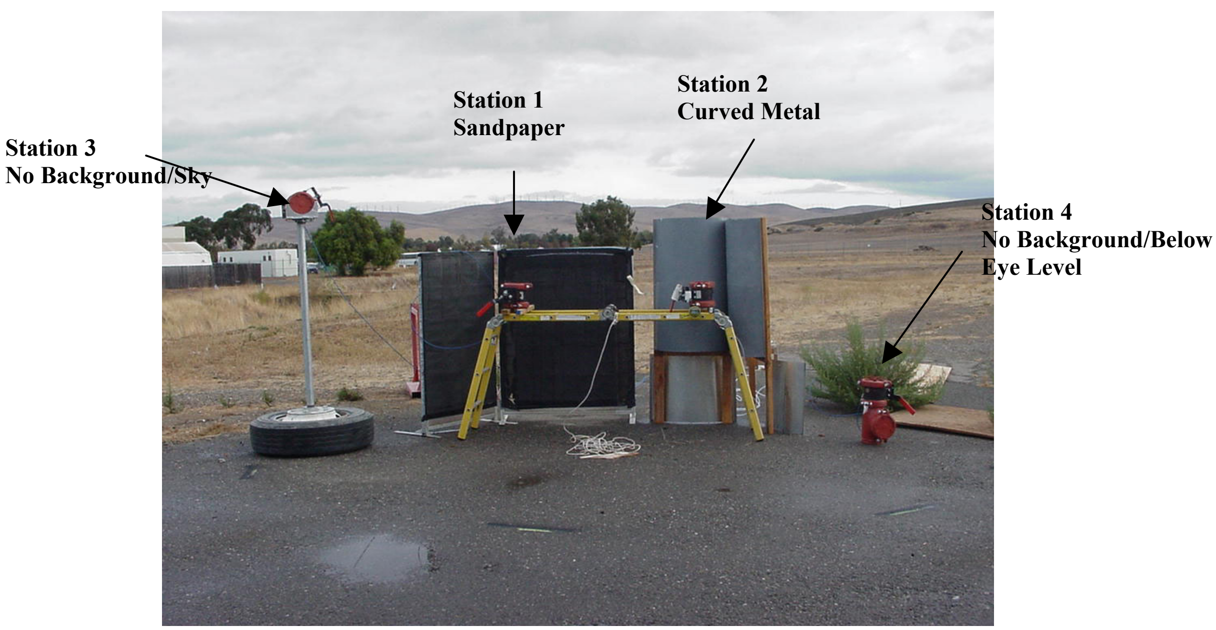

8.2 Laboratory Test Results

As expected, the mass rate detection threshold increased with increasing distance and windspeed for a given background. Figure 8-3 shows the detection thresholds for all test conditions. As is shown, with the exception of 10 cases, the mass rate detection threshold was below 10 g/hr. Seventy-three percent (73%) of the mass detection thresholds determined in the lab tests were below 5 g/hr.

8.3 Statistical Analyses of Test Data

A statistical analysis of the laboratory test data was conducted to determine an overall model to predict results using the optical imager.

8.3.1 Observed and predicted detection thresholds

The results for the overall model fitted to the wind tunnel test data for a curved metal background are shown in Figure 8-4. The best-fit statistical correlation of the data is a linear relationship on a semi-log curve of leak detection threshold versus windspeed. The curve predicts the leak values that would be detected 95% of the time under the given conditions. The model shows that from 3 meters away, with 1 meter/s windspeed (equivalent to ~ 2.2 miles per hour) the detection threshold of a leak that would be detected 95% of the time would be approximately 5 g/hr. A 60 g/hr leak would be detected 95% of the time from 3 meters distance with a 10 m/s (22 mph) windspeed.

Figure 8-4

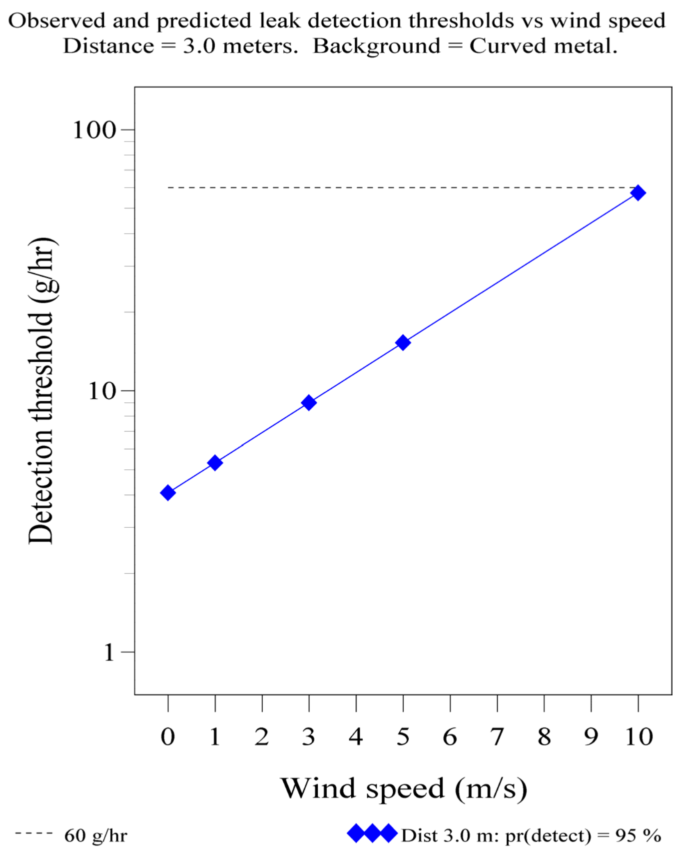

Figure 8-3. Mass Rate Detection Thresholds for Wind Tunnel & Roving Tests

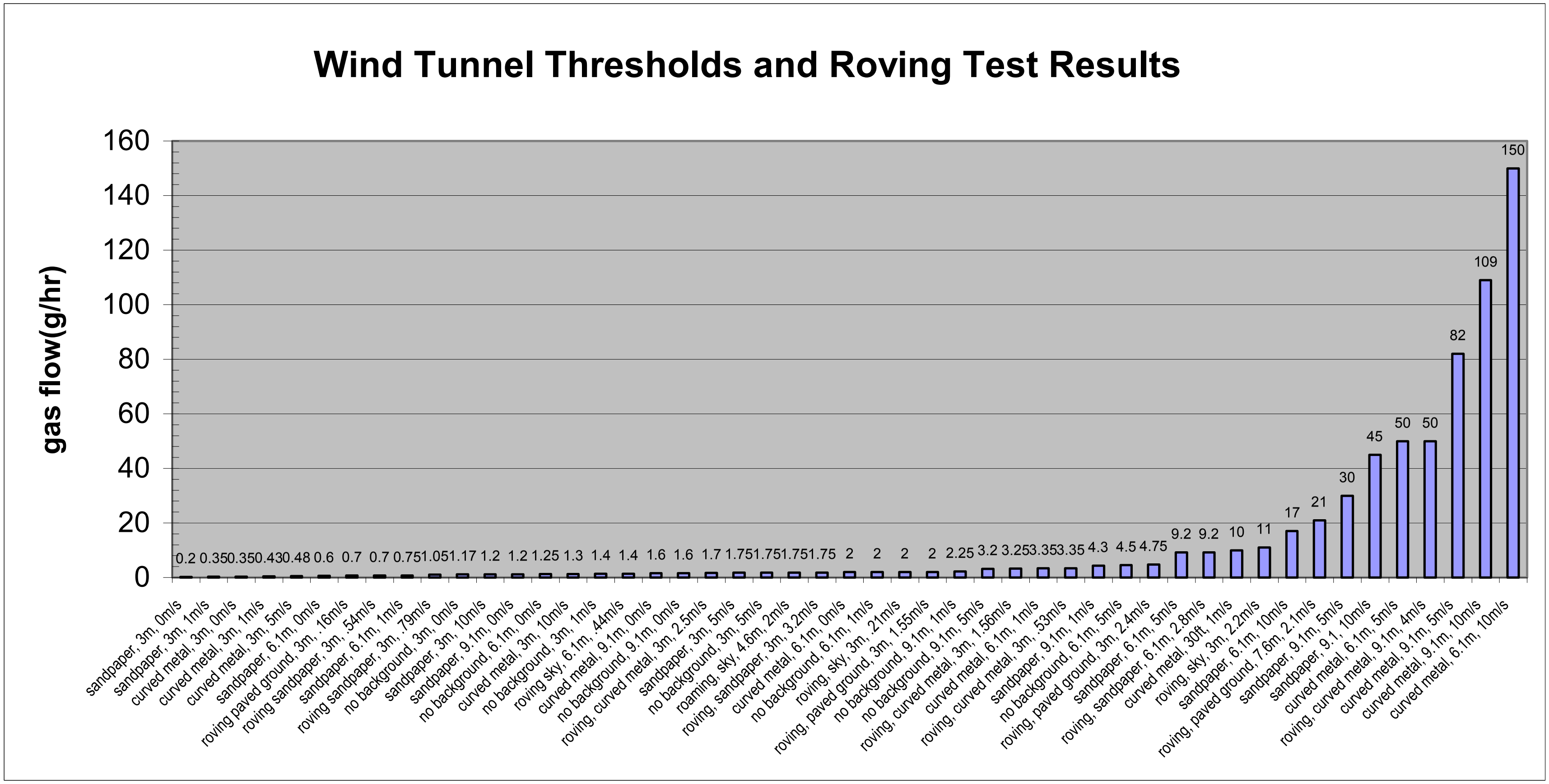

8.3.2 Predicted detection probabilities

Figure 8 - 5

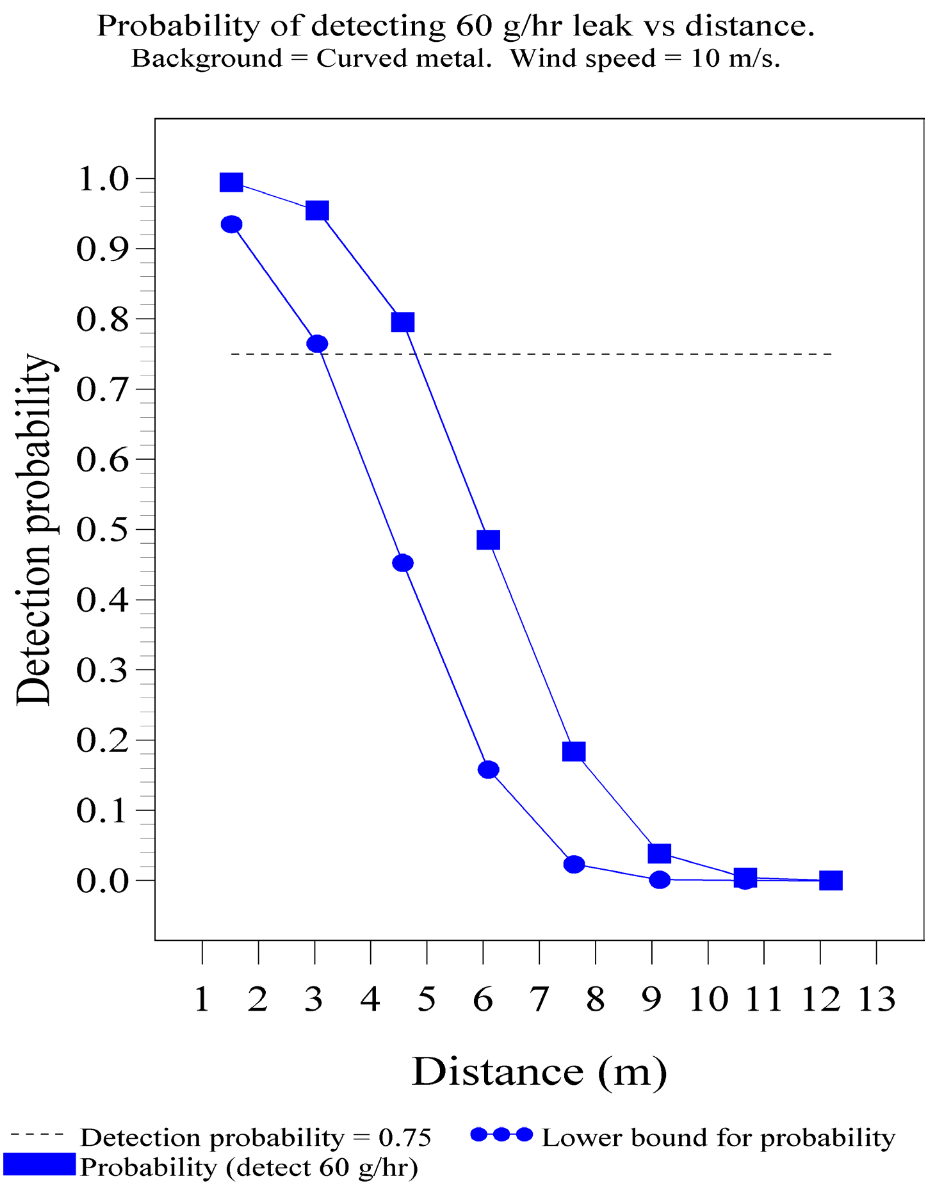

The statistical analysis determined the probability of detecting a 60 g/hr leak as a function of distance, wind speed, and background. The results of this analysis can be used to evaluate how well the device will perform under various conditions. Figure 8-5, is for curved metal background at a very high wind speed of 10 meters/s. Assume, for example, that the desired detection probability for curved metal background at a wind speed of 10 meters/s is 0.75. The dashed line at 0.75 intersects the probability curve, Pr(detect 60 g/hr),[9] at about 4.9 meters distance and intersects the lower bound curve at about 3 meters distance. Therefore, the model's best estimate of the maximum allowed distance is 4.9 m, but a more conservative value of 3 m would ensure with 95 % confidence that the detection probability is at least 0.75. Using the lower bound (3 m) rather than the point estimate (4.9 m) accounts for the uncertainties in the estimated model coefficients.

[9] Pr(detect 60 g/hr) =
$\Phi(\{\log(60) - [a1 \times S + a2 \times D{\times}S + a3 \times C + a4 \times D{\times}C + a5 \times N + a6 \times D{\times}N + a7 \times D{\times}W + a8 \times W{\times}S + a9 \times W{\times}C + a10 \times W{\times}N + a11 \times P + a12 \times D{\times}P + a13 \times W{\times}P]\} / \text{sigma})$,

where Φ is the standard normal cumulative distribution function.

8.2.3 Predicted distance or wind speed to detect a 60 g/hr leak

The statistical model also estimates the distance at which a 60 g/hr leak[10] can be detected 95 % of the time, for a given wind speed.

These maximum distance and wind speed values were calculated using the equation for Pr(detect 60 g/hr) and substituting the distance or wind speed values to make this probability equal to 95 % (see footnote 9 for equation for Pr(detect 60 g/hr)). The equation can be solved uniquely because the model is linear and increasing in both wind speed and distance. Figure 8-6 shows these results.

Assume that the desired detection probability for curved metal at a wind speed of 5 meters/s (11 mph) is 0.95. A vertical line through the wind speed of 5 meters/s intersects the maximum distance curve at about 6.1 m and intersects the lower bound curve at about 5.2 m. Therefore, the model's best estimate of the maximum allowed distance is 6.1 m, but a more conservative value of 5.2 m would ensure with 95 % confidence that the detection probability is at least 0.95. Using the lower bound (5.2 m) rather than the point estimate (6.1 m) accounts for the uncertainties in the estimated model coefficients.

Figure 8 - 6

Predicted distance at which probability of detecting 60 g/hr leak = 95 %, plotted against wind speed
Background = Curved metal

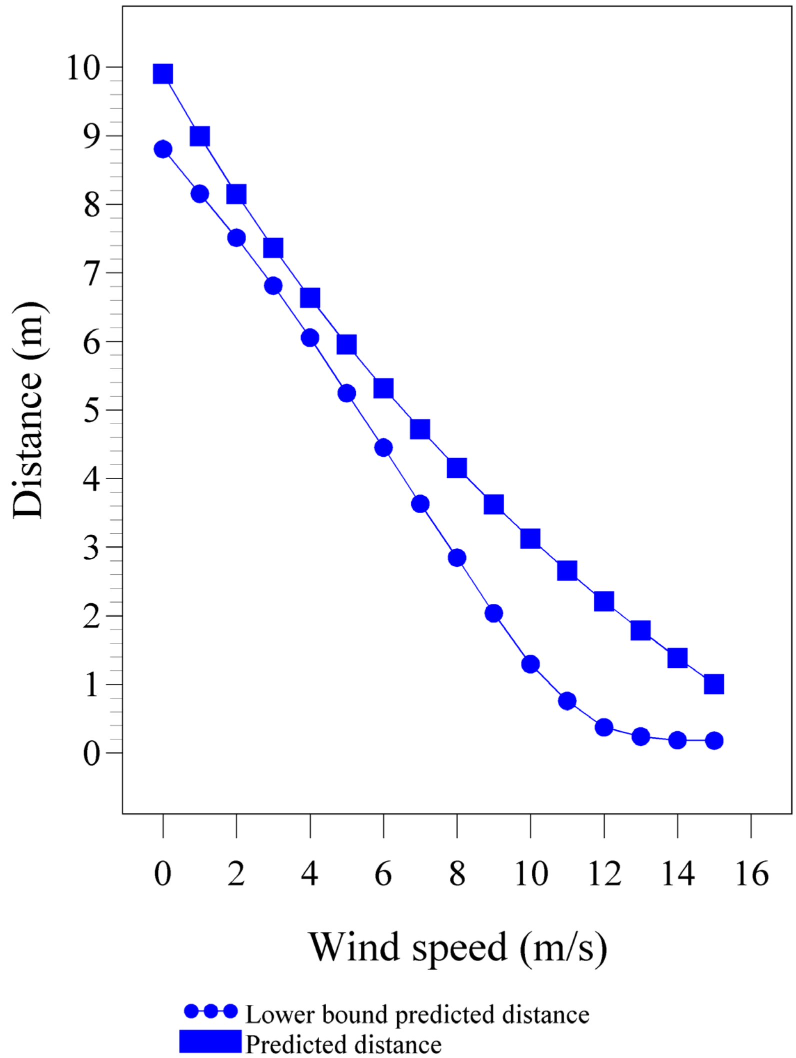

[10] The Monte Carlo analysis equivalent leak rate.

9.0 Refinery Test of Portable Fiber Laser

A field study was conducted at a refinery to evaluate the performance of a prototype portable fiber laser to detect fugitive emissions under normal operating conditions. Specific aims of the study were to:

- Demonstrate that the prototype portable BAGI device detects and successfully images fugitive emissions.
- Gather data that can be used to establish the mass-emission detection capabilities of the gas imaging technology.
- Gather data that can begin to establish the sensitivity of the BAGI technology to various factors that might be encountered during routine use at a refinery. Such factors include distance from scanned component, sight lines and angle-of-view, infrared backscatter and absorption properties of background components, weather conditions, and chemical composition of the emissions.

9.1 Study Methodology

Four process areas were monitored:

- Alkylation Plant (ALK)
- Saturated Gas Plant (SGP)
- Unsaturated Gas Plant (USGP)
- Isomerization Plant (ISOM)

The mass rates of several leaks detected by the fiber laser were determined using bagging techniques. The distance between the fiber laser and the leaking component was recorded, as was local wind speed in the vicinity of the leak. A brief summary of the conclusions and findings are presented below.

9.2 Study Conclusions, Data Analysis and Results

The study concluded that the prototype fiber laser can detect leaks of mixtures of olefinic and aliphatic hydrocarbons from LDAR and non-LDAR components at a rate of about 20 g/hr of total hydrocarbon and above under normal refinery operating conditions, against typical reflective surfaces found at a refinery.

Study Data

The field study collected data from 41 leak sources within four process areas. The screened process areas were: the Alkylation Plant, Saturated Gas Plant, Unsaturated Gas Plant, and the Isomerization plant. Thirty of the 41 leaks were detected in the Saturated Gas Plant (SGP); five (5) in the Unsaturated Gas Plant (USGP); and 6 leaks at the Isomerization Plant (ISOM). No leaks were found at the Alkylation Plant.

Twenty-eight of the 41 leak sources were bagged and analyzed for mass leak rate and chemical composition. Analysis of the bagged samples indicated that the leaks consisted of mixtures of hydrocarbons from C1 to C6 and above.

Performance of the Fiber Laser (Detected Mass Leak Rate)

Figure 9-1 illustrates the performance of the fiber laser in detecting mass leak rate (note: the Y axis is used just to separate the data sets for viewing results). As the plot illustrates, the fiber laser detected all bagged leaks above about 20 g/hr. Below about 20 g/hr the fiber laser missed 3 of the 12 recorded leaks (one each at SGP and USGP, and the third at the ISOM), and detected two known leaks (a 16 g/hr leak at USGP and a 0.12 g/hr leak at SGP) once a Styrofoam background was held behind the component.

Figure 9-1. Performance of Fiber laser (Detected Mass Leak Rates)

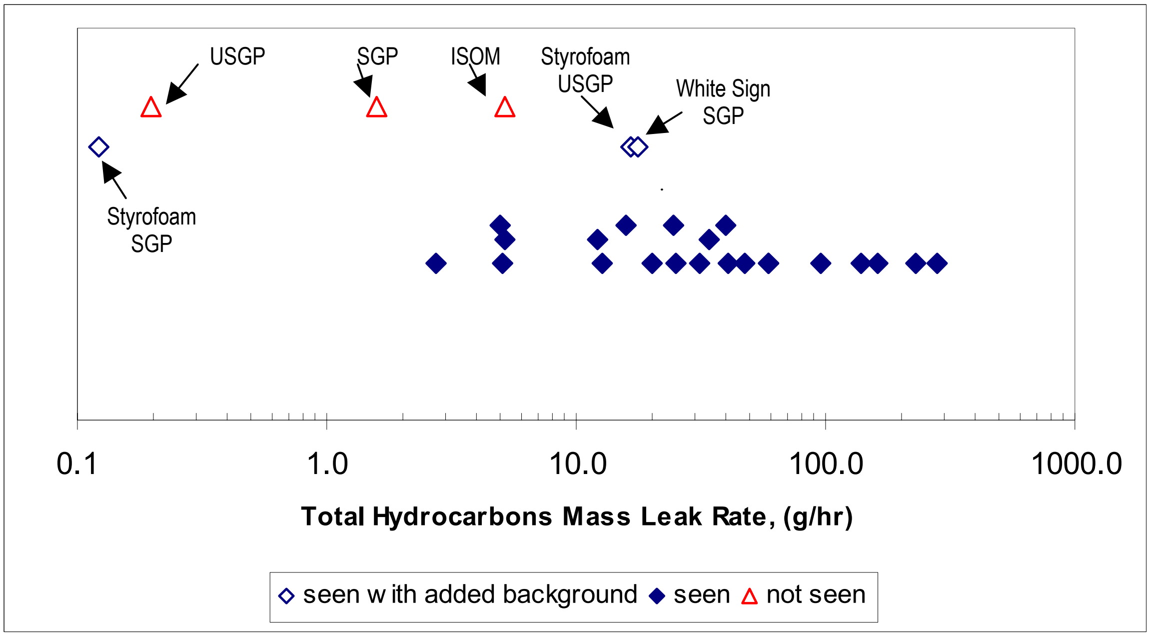

In one case at the SGP, an enamel white sign interfered with the reflection of the laser beam and the detection of the leak. If the operator changed position slightly, the leak became more visible. However, interference from the sign still occurred. The leak was made more visible using the Styrofoam background. Therefore, this leak is recorded as seen, with background.

In the two cases where the leaks became detectable once Styrofoam backgrounds were held behind the leaking components, the reason for originally "missing" the leaks appeared to be poor background.

Component Screening Rate

Analysis determined that the screening rate during the test was about 35 components per minute[11]. Using plant estimates, the total number of components monitored was estimated to be approximately 27,000 as shown in Table 9-1. This estimate includes counts for valves, pumps and connectors.

[11] Time spent scanning process areas during the test approximated 13 hours.

Table 9-1. Components Monitored During Test

Process Area	Component Count		Estimated % LDAR Components Scanned	Components Scanned		Estimated Connectors[a]	Totals
	Valves	Pumps		Valves	Pumps		
Alky Plant	2600	20	10%	**260**	**2**	**1,040**	***1,302***
UnSat Gas Plant	1700	24	25%	**425**	**6**	**1,700**	***2,131***
Sat Gas Plant	4600	45	75%	**3,450**	**34**	**13,800**	***17,284***
Isomerization Plant	2700	30	50%	**1,350**	**15**	**5,400**	***6,765***
				5,485	***57***	***21,940***	***27,482***

[a]4 times valves per plant guidance.

10.0 Testing the CO_2 Laser for Ethylene Monitoring

In 2002, Houston Area Advanced Research Center (HARC) commissioned tests at two olefin plants in Texas. The objectives of these tests were to:

- Conduct a demonstration of a portable optical gas imaging device in two industrial sites (ethylene and polyethylene producers) to evaluate the capability of the device in detecting fugitive emissions under normal chemical plant operating conditions;

- Identify, if possible, leaking equipment detected with the portable optical gas imaging device but listed as non-leaking when monitored under Method 21 procedures;

- Gather data that could be used to establish the mass emission detection capability of the portable optical gas imaging device; and

- Gather data that could begin to establish the sensitivity of the portable optical gas imaging device to various factors that might be encountered during routine use at a chemical plant including, but not limited to, distance from scanned components, sight lines and angle-of-view, infrared backscatter and absorption properties of background components, weather conditions, and chemical composition of emissions.

10.1 Study Methodology

The tests were conducted at two ethylene facilities in Texas[12]. Four process areas were monitored:

- Cold Ends
- Ethylene Product Pumps & Heater
- Compressors
- Drying Area

Mass rates of several leaks detected by the CO_2 laser were determined using bagging techniques. The distance between the CO_2 laser and the leaking component was recorded, as was local wind speed in the vicinity of the leak. Brief discussions of the conclusions and findings are presented below.

[12] Referred to as Site A and Site B.

10.2 Study Findings

The primary conclusions and supporting findings from this effort were as follows:

1. The CO_2 laser was able to identify leaking components while monitoring under normal petrochemical plant operating conditions and good weather conditions (light wind, clear sky, summer temperatures).

   - All leaks above about 1g/hr were detected by the CO_2 laser. (See Figure 10-1).
   - Ethylene was the only species examined during testing at both sites.

Figure 10-1. CO_2 Laser Performance at Ethylene Facilities

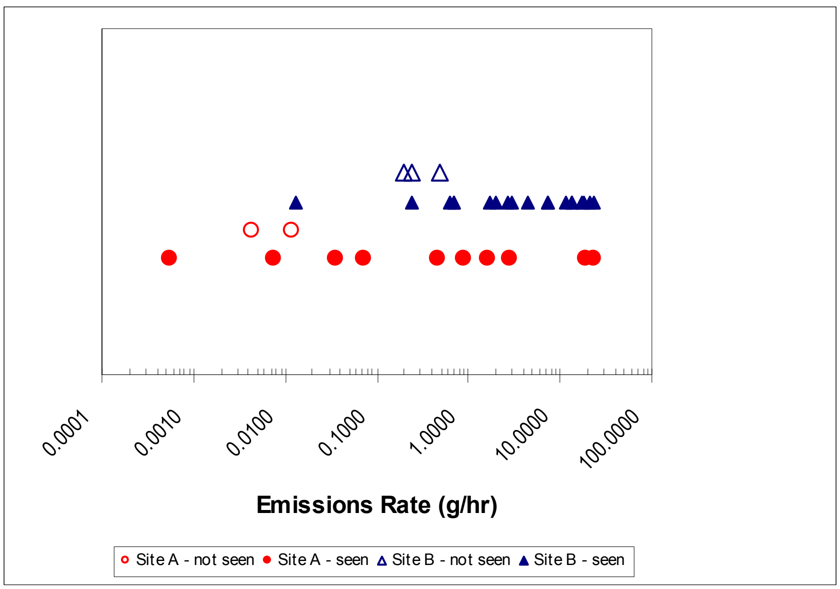

   - Method 21 techniques sometimes inaccurately attribute leaks. Several components tagged for repair were found not to be leaking. Instead, the CO_2 laser determined that the tagged components were in the path of the plume emanating from another (often, overlooked and hence untagged) component. As the wind direction changed these tagged "non-leaking" components are no longer in the plume's path, and were found not to be leaking. Plant personnel at one site indicated that they have, on many occasions, detected and tagged components for repair, only to find no leak at the component on a later date when a crew arrives to perform repairs.

2. The majority of components detected as leaking had screening vales above 10,000 ppmv. This result is in keeping with trends seen in API's 1997 study of refinery LDAR data.

   - Approximately 97% of the 95 detected leaking components at Site A and 83% of the 52 detected leaking components at Site B had screening values over 1,000 ppmv. Approximately 63% of Site A's and 52% of Site B's detected leakers had screening values over 10,000 ppmv.

Bibliography

[1] American Petroleum Institute, "*Analysis of Refinery Screening Data,"* Publication # 310, Washington, DC, November 1997.

[2] ICF Consulting, *Compendium of Sensing Technologies to Detect and Measure VOCs and HAPs in Air*, Washington, DC, June 1999

[3] McRae, T. G. and Kulp, T. G., "Backscatter Absorption Gas Imaging: a New Technique for Gas Visualization" Applied Optics, 1993, Vol. 32, 4037-4050.

[4] Gas Research Institute (GRI), *"Evaluation of the GRI Gas Imaging Leak Survey System,"* GRI-98/0014, February 1998

[5] McRae, Tom, *"GasVue VOC and SF6 Leak Location Field Test Results,"* Proceedings of the Society of Photo-Optical Instrumentation Engineers (SPIE) Conference on Environmental Monitoring and Remediation Technologies II, SPIE Vol 3853, Boston MA, September 20-22, 1999

[6] Epperson, David. L., Siegell, Jeffery, H., *"Equivalent Leak Levels & Monitoring Frequencies for Smart LDAR,"* Valve World 2002, November, 2002

Additional copies are available through Global Engineering Documents at (800) 854-7179 or (303) 397-7956

Information about API Publications, Programs and Services is available on the World Wide Web at http://www.api.org

American Petroleum Institute
1220 L Street, Northwest
Washington, D.C. 20005-4070
202-682-8000

Product No: I0LDAR